Title
Role of Necroptosis in T Cell Activation

Author
Zhao, Zhanran

Publication Date
2018

Peer reviewed|Thesis/dissertation

Role of Necroptosis in T Cell Activation

by

Zhanran Zhao

A dissertation submitted in partial satisfaction of the

requirements for the degree of

Doctor of Philosophy

in

Molecular and Cell Biology

in the

Graduate Division

of the

University of California, Berkeley

Committee in charge:

Professor Astar Winoto, Chair
Professor Ellen Robey
Professor Lin He
Professor Danica Chen

Summer 2018

Abstract

Role of Necroptosis in T Cell Activation

by

Zhanran Zhao

Doctor of Philosophy in Molecular and Cell Biology

University of California, Berkeley

Professor Astar Winoto, Chair

Necroptosis is a programmed cell death pathway characterized by a necrosis-like morphology and mediated in part by the kinase activity of receptor-interacting protein kinase 3 (RIPK3) and, in most cases, its partner RIP1 as well. Necroptosis is a hidden cell death pathway, as it was initially only described in cells deficient in FADD or caspase-8. Necroptosis has been shown to play important roles in injury, disease models, and, more recently, in certain viral infections. However, its role in a normal physiological setting is still not completely clear. Using Nec-1, an inhibitor of RIP1 kinase activity, we have previously shown that a proportion of CD8 T cells can be rescued from cell death induced by TCR activation *in vitro*. This observation led us to characterize the phenotype of T cells from mice deficient in RIP3 to examine the role necroptosis plays in T cell activation. We found that inhibiting necroptosis can lead to increased cell number and activity of cytotoxic T lymphocytes (CTLs). Furthermore, *Rip3*$^{-/-}$ mice showed improved tumor responses compared to littermate controls, with decreased expression of inhibitory markers on CTLs and reduced suppressive Treg populations in the tumor infiltrating lymphocytes. Using adoptive transfer, we showed that this effect is primarily driven by *Rip3*$^{-/-}$ T cells and that these T cells exhibit elevated activation activities and improved anti-tumor function. Necroptosis thus helps to regulate T cell activation to maintain the delicate balance of immune homeostasis.

DEDICATION

To my great grandmother, who showed me who I'm not but can try to be

ACKNOWLEDGEMENTS

Thank you, Astar, for everything.

Thank you, the members of my thesis committee – Ellen, Lin, and Danica – for your insightful comments, incredibly helpful suggestions, and kind guidance.

Thank you, my undergraduate students, Winnie and Emily, for your hard work and putting up with me day in and day out.

Thank you, everyone else in the Winoto lab, past and present, whom I've had the great fortune to work with, for your invaluable inputs, aid with my experiments (especially Yuefang – thank you for dealing with all those long hours of injections), and support.

And last but not least, thank you, Karl, for – in the best way I can put this– joining the lab with me six years ago, something that I'm always and still will be thankful for – for a long time to come.

TABLE OF CONTENTS

GENERAL INTRODUCTION

General Introduction

The activation of naïve T cells is an intricately regulated process that involves the interplay between and control of proliferative and programmed cell death (PCD) pathways to maintain a balanced immune response – one just strong enough to eliminate a foreign invader but not so strong as to inflict bystander damage to the host. Regulation of the T cell response is crucial for the prevention of autoimmunity and the formation of immunological memory. In recent years understanding of this regulation has allowed for manipulation of some of these pathways to use as treatments in diseases, including cancer[1,2].

T cell activation consists of distinct phases, beginning with engagement of the T cell receptor (TCR) and initial expansion followed by contraction and generation of memory[3]. After recognition of cognate antigen bound to MHC through the TCR, naïve T cells proliferate and upregulate death receptor members of the tumor necrosis alpha receptor (TNFR) superfamily (including TNFR1 and Fas/CD95) that help to limit their expansion through extrinsic apoptosis (**Fig A**). Extrinsic apoptosis requires adaptor molecules such as Fas-associated death domain (FADD) to recruit and help activate procaspase-8, which then results in the induction of other caspases to drive apoptosis[4]. Thus, deficiency of FADD or caspase-8 may be expected to have profound effects on T cell survival upon activation. Indeed, knockout of either of these proteins in T cells results in a severe defect; however, rather than protecting the cells from apoptosis, FADD or caspase-8 deletion instead led to a dramatic increase in cell mortality[5,6]. Furthermore, the dying cells adopted a necrosis-like morphology.

This observation is reminiscent of the phenotype, originally described in Jurkat cells treated with TNFα in the presence of the caspase-8 inhibitor zVAD-fmk, of increased cell death upon inhibition of extrinsic apoptosis[7]. A small molecule screen for suppressors of this death identified Necrostatin-1 (Nec-1), which blocks the kinase activity of receptor-interacting protein kinase (RIP1 or RIPK1), a molecule that is typically recruited to the death receptor signaling platform along with FADD and plays important roles in NF-κB activation downstream of TNFR1[8]. This death was termed "necroptosis".

Therefore, necroptosis can be thought of as a controlled form of necrosis that has the immunological and physiological implications of necrosis such as inflammation but retains some of the regulation of more conventional PCD pathways such as apoptosis. We in the lab have previously demonstrated necroptosis may be important for controlling naïve T cell proliferation upon TCR activation in T cell conditional FADD knockout ($tFADD^{-/-}$) mice. Nec-1 addition to activated $tFADD^{-/-}$ T cells was able to rescue the survival defect of these cells and allow for normal proliferation, suggesting that necroptosis is indeed responsible for the increased mortality. Interestingly, Nec-1 addition resulted in improved survival of the wild-type control T cells as well, with a particularly pronounced effect in the CD8 proportion[6].

Necroptosis requires the formation of an amyloid-like structure termed the necrosome formed by the attachment of RIP1 with another member of the same protein family, RIP3, at their homotypic RHIM domains, which in turn leads to the activation of an effector protein mixed lineage kinase-like (MLKL) at the mitochondria to trigger death by translocation to puncturing of the plasma membrane[9,10]. Further confirming the role of necroptosis in T cell biology, we showed that mice lacking RIP3 show increased T cell proliferation compared to wild-type heterozygous littermates upon stimulation, also with a more prominent phenotype in the CD8 compartment compared to that of the CD4. These data collectively suggest that necroptosis may be triggered as a normal physiological response upon naïve T cell activation.

One setting in which necroptosis may play a crucial role in regulation of the T cell response is cancer. Treatments with antibodies against the T cell activation inhibitory molecules CTLA-4 or PD-1/PD-L1 alone or in combination with each other as well as other therapies targeted at the immune response have shown to be more effective at controlling certain types of tumors than conventional treatments[11–14]. As necroptosis also appears to be an inhibitory pathway of T cell activation *in vitro*, we were interested in studying the impact of suppressing this pathway *in vivo* on T cell response against tumors. Rescuing CD8 T cells from necroptosis will perhaps allow for a more potent anti-tumor response and better control against specific tumors.

Necroptosis and the role of RIP3

As is the case with apoptosis, necroptosis can be turned on downstream of multiple inducing signals, including but not limited to cell damage, death ligands, and, most importantly in the context of the immune system, infection[15–18]. Originally necroptosis was described as a backup pathway to apoptosis and appeared to be only triggered in the absence of components of the extrinsic apoptotic pathway like caspase-8 or FADD. Thus, the two pathways are intricately linked and extensively cross-talk with each other.

In extrinsic apoptosis, members of the TNFR superfamily are activated to trigger caspase dependent cleavage of intracellular contents upon ligation of a death ligand such as TNFα[19]. In the case of the TNFR1 pathway, binding of TNFα to its receptor leads to receptor auto-trimerization and the assembly of a signaling platform consisting of adaptor molecules such as TNFR1 associated death domain (TRADD) and FADD to help recruit procaspase-8[20]. Procaspase-8 dimerizes and self-cleaves to generate active, mature caspase-8 which acts through Bid and caspase-3 to execute apoptosis, causing proteolysis, chromosome condensation, and eventual cell fragmentation and breakage[21,22]. The self-cleavage of procaspase-8 can be further regulated by caspase-8 and FADD-like regulator (CFLAR or c-FLIP). Distinct isoforms of c-FLIP can bind to procaspase-8 in place of another molecule of procaspase-8 in the dimer to inhibit its self-cleavage and prevent or at least raise the threshold for apoptosis[23–26].

The assembled signaling complex downstream of TNFR1 ligation represents a crucial decision point in cell fate – to survive or to die, and if the latter, in what manner of cell death. In addition to recruiting procaspase-8, the adaptor molecules TRADD and FADD can associate with RIP1 via homotypic interactions through their shared death domains. The ubiquitination of RIP1 regulates the switch between life and death and apoptosis and necroptosis. Lysine 63 linked polyubiquitin chains on RIP1 allow for binding of NF-κB essential modulator (NEMO) to activate NF-κB and promote cell survival and growth while deubiquitination permits RIP1 to associate with procaspase-8 and induce apoptosis[27–29].

When TNFα was added along with the caspase-8 inhibitor zVAD-fmk to Jurkat cells, the cells underwent massive cell death instead of surviving the treatment, suggesting that caspase-8, in addition to its pro-apoptotic role, also has a protective function. The conflicting role of caspase-8 was elucidated upon treatment with Necrostatin-1, a small molecule inhibitor of the kinase activity of RIP1, which led to almost complete rescue. Ablation of FADD was shown to have a similar death inducing effect in Jurkat cells and was also rescued by inhibiting RIP1[30]. Caspase-8 and FADD therefore suppress necroptosis mediated by RIP1's kinase activity, suggesting that necroptosis may be a back-up PCD to apoptosis that is initiated when apoptosis is inhibited, by a pathogen, for example, or a mutation in a tumor cell.

In the absence of caspase-8 or FADD, the apoptotic complex is converted into a necroptosis inducing platform instead, in which RIP1 now interacts with RIP3, leading to the phosphorylation of both proteins through their kinase domains to activate MLKL. A recently identified ubiquitination site on human RIP1, K115, seems to play a role in necroptosis induction, as mutation of the site dampens RIP1's necroptotic kinase activity and prevented cell death[27].

While RIP1 and RIP3 are critical in most scenarios of necroptosis, a great deal of diversity exists in the regulation and activation of the kinase activities of these two proteins. Pattern recognition receptors like TLR3 and TLR4 may recruit RIP3 via its RHIM domain through the adaptor molecule TRIF to trigger necroptosis in response to infection[31]. Genotoxic stress can lead to the spontaneous assembly of a RIP1, RIP3, FADD, and caspase-8 complex called the ripoptosome independent of receptor ligation. While in recent years we have a developed a general understanding of the mediators and some important regulators of necroptosis, much of how it is controlled in various cell types, how it interacts with other pathways, and, importantly, how it can be activated in a physiological setting in which caspase-8 and FADD are present are all questions that still have unclear or incomplete answers.

Cell death in T cell activation

Cell death plays a critical role in maintaining immune homeostasis upon naïve T cell activation. Only a minority of activated T cells survive this phase, termed contraction, to become memory cells. Contraction is thought to be primarily due to apoptosis mediated by bim or death receptors such as Fas. Indeed, FasL is upregulated upon T cell activation by IL-2 to complete a negative feedback loop that helps to limit the initial immune response[32,33].

The control of T cell contraction remains a black box, partly due to its rapid kinetics and the lack of appropriate models for study *in vivo*. Antigen stimulation duration and strength, T cell population size, competition for cytokines and growth factors in the niche, and cell fate (whether an activated T cells is predetermined to become an effector or a memory cell) have all been proposed to play a role in regulating the onset and magnitude of contraction[34–37]. Despite extensive study, however, the nature and timing of the signals that initiate contraction elude clear description.

The presence of antigen may affect this timing. A FRET reporter bone marrow chimera for caspase-3 activation demonstrated that sustained antigen stimulation early in T cell activation can delay the initiation of cell death *in vivo*[38]. This evidence suggests that induction of cell death during contraction is a plastic event sensitive to changes in the environment and not a pre-programmed event determined by initial activation of the TCR. In line with this data, both T cells associated with an effector and a memory expression profile (IL-7Rα^{lo} KLRG-1^{hi} and the reverse, respectively) are equally sensitive to contraction[39]. Remarkably, rescue of the former from cell death may lead to its eventual differentiation into a memory cell. Thus, the question of what the immediate upstream signals that trigger T cell contraction are becomes more important.

Although apoptosis is the major mechanism mediating contraction, other PCD pathways, including necroptosis, may contribute to the cell death. Wild-type T cells stimulated with α-CD3/CD28 antibody *in vitro* show improved survival 120 hours post-activation, which coincides with the onset of contraction[6]. However, this defect can be rescued when by crossing the mice to RIP3 knockouts or by treating the T cells with Nec-1. These results suggest that T cells are certainly capable of initiating necroptosis and, indeed, within 24 hours post-stimulation, T cells begin to express considerable amounts of RIP1 and RIP3 and interaction between the pair of

kinases can be detected by co-immunoprecipitation[40]. Whether T cell necroptosis is relevant in a physiological setting remains to be addressed.

A further and a more basic question of the role of necroptosis in T cells is how to reconcile the pro-inflammatory consequences of a necrosis-like cell death with the purpose of contraction – to downregulate the immune response. The ability of T cells to undergo necroptosis post-activation in the absence of apoptotic mediators may suggest that this pathway is a further step to limit T cell activation and may be important in case apoptosis is somehow compromised, as in the case of infection by certain viruses that encode apoptotic inhibitors. Therefore, transient blocking of necroptosis during T cell activation may be useful for rescuing effector T cells and can be used as a tool for counteracting immunosuppression in settings like cancer.

T cell function in tumors

The intimate and often conflicting relationship between tumor cells and T cells has been extensively studied in the past two decades and the methods T cells rely on for extermination of cancer cells and the tactics cancer cells employ to impede, evade, and hijack these methods have shed intense light on previously dark corners of tumor and T cell biology. Though the phenomenon of immunosurveillance, the detection of aberrant tumor antigens by the adaptive immune response, was long proposed, the striking phenotype observed in so-called RkSk mice deficient in RAG2 and STAT1 of increased susceptibility to tumors cemented the importance of the adaptive immune system for tumor control[41].

This initial observation paved the road for extensive investigation into the cross-talk between the developing tumor and the immune system and led to the postulation of the immunoediting hypothesis of elimination, equilibrium and escape to explain the confounding observation that in tumors often reside a substantial, tumor-specific T cell population[42]. Some of the pathways that tumors use to downregulate the T cell response, such as the programmed death-1 (PD-1) and cytotoxic T-lymphocyte associated-4 (CTLA-4) signaling cascades, are utilized by the immune system during the course of a normal response to prevent excessive activation or to protect against autoimmunity. However, tumors hijack these molecules to dampen or suppress a productive CTL response to cancer and thereby progress. Blockade of these inhibitory receptors on T cells or ablation of the expression of their ligands on tumor cells with antibodies can restore proper T cell responses against many types of tumors and have proven to be effective in the clinic[43–45].

In the tumor microenvironment, elevated numbers of T regulatory cells can often be detected. Though sharing some similar functions, these Treg populations are heterogeneous, with some recruited by the tumor from surrounding lymph nodes and some converted from conventional T cell lineages through cytokines secreted by tumor associated cells in the tumor microenvironment (TME), and may help to impede T cell detection and elimination of the tumor. In particular, these Tregs suppress the CD8 response by upregulation of some of the inhibitory markers described above, release of suppressive cytokines such as TGF-beta that may also play a dual role in aiding the tumor in colonizing distant sites, and general inhibition of proliferation and induction of apoptosis in effector CD8 T cells[46–48]. The exhausted and anergic phenotype of CTLs in the TME resemble those described in autoimmune and chronic infection models and further provide explanation for the observation that although tumor specific T cells are present, they have been rendered impotent by cell types and molecules in the TME[49–51].

Thus, T cells, in particular CTLs, play a crucial role in tumor control as they are responsible for the detection of tumor specific antigens and subsequent elimination of tumor

cells and for a tumor to progress it must escape from surveillance by the adaptive immune response. Rescuing these exhausted or repressed T cells in the tumor environment may therefore represent an effective method of cancer treatment. Indeed, blocking antibodies against PD-1 and CTLA-4 restore T cell function, as indicated by elevated expression of various activation markers and downregulation of inhibitory molecules on the cell surface[52,53]. These restored T cells also demonstrate increased secretion of effector cytokines, such as TNFα and IFN-γ[54]. In addition to their direct effects on CTLs, anti-PD1/PD-L1 and anti-CTLA-4 blocking antibodies have also been shown to modulate the TME through recruitment and recovery of CTL function, resulting in a more productive surrounding for proper activation of tumor specific T cells and generation of a sustained immune response to the tumor.

The role of necroptosis in T cell activation and function

Given the importance of cell death in helping to shape the T cell response and the potential role that programmed necrosis may play in the process, we were interested in understanding what may occur when necroptosis is blocked in T cells. To that end, we obtained mice deficient in RIP3 and analyzed the behavior of T cells from these mice upon activation *in vitro* as well as in tumor models. We also used these T cells to help understand the biochemical pathway that regulates this process.

We show here that necroptosis plays a crucial role in limiting T cell numbers upon activation and that blocking this inhibition of T cell survival we are able to rescue a large number of functional CD8 T cells that in turn seem to be able to protect against challenge with tumors *in vivo* in subcutaneous tumor models. We demonstrate that this control is due to the enhanced survival of these T cells and not due to elevated activation or other effects that necroptosis plays on T cell function. We also reveal that this phenotype is sufficiently potent and intrinsic that it can be transferred from animal to animal and that knocking out RIP3 may prove to be another avenue that, in combination with other treatments, can be useful for treatment of various tumors.

FIGURE LEGENDS
Figure A

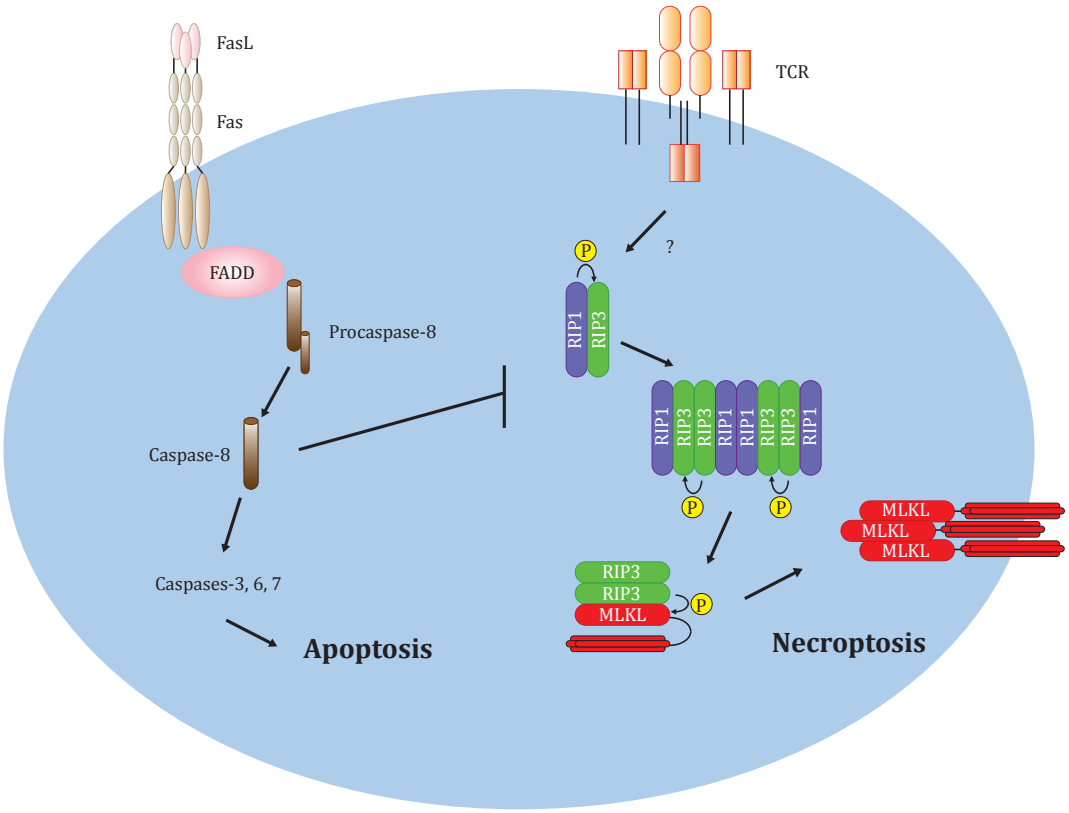

Figure A Pathways of programmed cell death in activated T cells. TCR stimulation of naïve T cells leads to rapid proliferation, which is followed by sharp contraction through programmed cell death pathways, including apoptosis and necroptosis. Fas is upregulated by IL-2 from activated T cells, forming a negative feedback loop to limit proliferation. Receptor ligation recruits caspase-8 through FADD, and allows it to cleave other caspases to drive apoptosis. Alternatively, phosphorylation of RIP3 by RIP1 after TCR stimulation leads to the formation of an amyloid-like structure, which helps RIP3 phosphorylate MLKL. Active MLKL translocates to and forms pores in the plasma membrane, resulting in necroptosis. Genetic studies in mice have shown FADD and caspase-8 limit necroptosis in T cells, presumably by preventing the interaction between RIP1and RIP3. The exact mechanism however remains unclear.

Chapter 1: Regulation of T cell survival by programmed necrosis and the effects of blocking necroptosis on T cell function

Introduction

CD8 T cells are crucial mediators of antitumor immunity. Recognition of tissue specific antigens or neoantigens on tumors by cytotoxic T lymphocytes (CTLs) can drive a potent antitumor response; however, the presence of CTLs in the tumor microenvironment alone does not necessarily predict tumor control[52]. The existence of a non- or weak functioning tumor specific CTL population in progressive tumors is a result of immune suppression by the tumor, which can take a variety of forms, including hampering of antigen presentation, upregulation of inhibitory ligands and cytokines, and induction of apoptosis of tumor infiltrating lymphocytes (TILs)[55,56]. These modes of suppression can lead to an anergic or exhausted T cell response and promotion of tolerance to tumor antigens rather than proper priming and activation of tumor specific T cells[50]. Antigen presentation, in particular that mediated by dendritic cells (DCs), plays a critical role in the decision between anergy and priming. CD4 as well as CD8 T cells isolated from tumors have been shown to be poor in proliferative and cytolytic ability upon stimulation by tumor antigens, presumably because the immunosuppressive nature of the tumor microenvironment, rich in cytokines such as IL-10 and vascular endothelial growth factor (VEGF), fails to provide the proper context for presentation by DCs, leading to induction of tolerance to the tumor rather than clearance[57,58].

In addition to inhibiting T cell activation and function through antigen presenting cells (APCs), tumors can also recruit immunosuppressive T regulatory (Treg) cells to promote inhibition of CTL activity[47]. Upon recruitment or conversion from conventional T cells, Tregs can proliferate and expand in the tumor to generate and sustain a potent immunosuppressive environment[59]. This heterogeneous population can in multiple ways impede the ability of CTLs to recognize and eliminate tumor cells. For example, secretion of inhibitory cytokines like TGF-β by Tregs dampens the expression and secretion by CTLs of cytolytic proteins such as perforin crucial for cytolysis[60]. Recently, a major research focus in cancer immunology has been inhibitory immune checkpoint proteins such as CTLA-4 and PD-1. Tregs co-opt a variety of these molecules, which help to limit excessive T cell expansion and activation in the course of a stereotypical adaptive immune response, to suppress antitumor activity of tumor specific CD4s and CD8s. CTLA-4 is expressed on Tregs and preferentially binds to the CD80/CD86 co-receptors while PD-L1 can be expressed on Tregs as well as tumor cells and binds to PD-1 to prevent proper activation and function of T cells respectively[61]. Blocking antibodies to these ligands or their receptors are able to restore CTL activity in the tumor environment, as shown by elevated expression of activating and effector markers and secretion of cytolytic cytokines, and demonstrate efficacy against multiple cancers, including melanoma, kidney, bladder, and some lymphomas, in the clinic[62]. α-CTLA-4 treatment may also directly inhibit the function of Tregs as Treg specific CTLA-4 knockout display systemic inflammation[63]. Thus, given the importance of CD8 T cells in antitumor protection and the evidence that targeting these cells may be an efficient avenue of tumor treatment, we are interested in understanding the fundamental regulation of CD8 function to better develop and design improved immunotherapies.

Programmed cell death (PCD) is a key pathway in maintaining T cell homeostasis and function[64]. Recognition of an antigen by naïve T cells results in a rapid initial expansion but, just as rapidly, the majority of T cells produced subsequently die through PCD, leaving only a small portion of activated T cells to go on to become memory T cells. Extrinsic apoptosis through

death receptors of the TNFR superfamily contributes to a majority of this death; however, necroptosis may also play a role in this process as addition of Nec-1 can lead to increased CD8 T cell numbers at late time points[6]. However, as Nec-1 can also inhibit other kinases, pathways other than necroptosis cannot be ruled out[65].

Necroptosis is thought of as a "hidden" or "back-up" pathway that is typically revealed only when FADD or caspase-8 is deleted or their activities are compromised or under some circumstances when the cell is under stress due to DNA damage or infection by certain viruses[66,67]. Recent studies have demonstrated that the formation of a complex between RIP1 and RIP3 is important for activation of necroptosis in T cells and that this interaction can be regulated at the level of RIP1 ubiquitination downstream of TCR activation[40]. However, the impact of this pathway on T cell function is still not well-understood. In particular, we are interested in understanding its role in CD8 biology in a tumor setting and the potential for exploiting T cell activation induced necroptosis for immunotherapy.

We used mice lacking RIP3 to study the effects of blocking necroptosis on T cell function, particularly on CTLs. We first sought to characterize *in vitro* changes in the activation and activity of CTLs from RIP3 knockout mice. We then aimed to describe the immune response in these animals to challenge with various tumor models. We were also interested in whether this response could be transferred by relaying the T cell compartment from animal to animal. Finally, we were curious as to the efficacy of combining conventional immunotherapies with inhibition of necroptosis on tumor protection.

Overall, we show here that CTLs from RIP3 knockout mouse display enhanced cytotoxicity both *in vitro* in killing assays and *in vivo* in the tumor microenvironment. This elevated activity may be due to the greatly increased numbers of RIP3 knockout CD8s remaining post-activation compared to wild-type. As a result, RIP3 knockout mice have improved tumor control and increased survival. This protection is also transferrable by adoptive transfer of activated CTLs from RIP3 knockout to wild-type animals. Thus, we demonstrate inhibition of T cell activation induced necroptosis can lead to an improved antitumor immune response and may be a novel therapeutic approach to tumor treatment.

Materials and Methods

T cell proliferation assay

Spleen and lymph nodes of 6-12 week old B6 wild-type or *Rip3*$^{-/-}$ mice were harvested, filtered into single cell suspensions, and RBC lysed. T cells were purified by CD3 column enrichment (R&D Systems) per manufacturer instructions and resuspended to $1x10^6$ cells/mL. 100 µL of purified T cells was added per well of a 96 well U-bottom plate pre-coated the night before at 4°C with 2 µg/mL of CD3 and CD28 antibody (UCSF). Nec-1/Nec-1s was added at 30 µM (Abcam) as indicated. Additional media was supplemented at 48, 72, 96, and 120 hrs post stimulation to sustain the culture. No exogenous IL-2 was added at any point during culture. Live cell counts by Trypan blue staining were collected every 24 hrs. Cells were also stained after counting for various activation markers, including live/dead dye (Tonbo), CD4, CD8, CD44, CD62L, CD69, and PD-1 (BD), then analyzed by flow cytometry.

CFSE

Purified T cells were resuspended to $10x10^6$ cells/mL after CD3 column enrichment and incubated with 10 µM CFSE diluted in PBS supplemented with Ca^{2+}/Mg^{2+} for 10 minutes at

37ºC. Cells were then washed four times with cRPMI and stimulated with 2 µg/mL plate-bound CD3/CD28 antibody. Analysis of CFSE dilution was carried out over the course of one week and cells were harvested every 24 hours for flow analysis during the time course.

Tumor injection
MCA-303 cells were collected, washed three times with PBS, and resuspended to a concentration of $5x10^5$ to $1x10^6$ cells/mL in sterile PBS. Six to twelve weeks old B6 or *Rip3*$^{-/-}$ mice were anaesthetized in an isoflurane chamber and shaved on the right flank. 100 µL of tumor cells were injected subcutaneously. Mice were monitored daily and tumor sizes were collected every two days or upon significant change from the previous day. Experimental endpoint was defined as a tumor size above 1000 mm^3 or upon ulceration of the tumor.

Tumor flow cytometry analysis
Spleen, non-draining/draining lymph nodes, and the tumor infiltrating lymphocyte (TIL) samples were collected and dissociated into single cell suspensions. Tumors were digested with collagenase type IV (Sigma) for 30 min at 37°C. Cells were either immediately stained with myeloid and lymphoid markers (CD45, CD11b, CD11c, F4/80, Ly6C, CD3, CD25, FoxP3 (BD)) or reactivated with tumor lysate or PMA/Ion overnight then stained intracellularly for various cytokines (TNF-alpha, IFN-gamma, CD107a, Granzyme B (BD)). Samples were fixed by either BD Cytofix (BD) or FoxP3 transcription factor staining buffer (eBioscience) and analyzed by flow cytometry.

Redirected lysis assay
P815 mastocytoma cells (ATCC) were washed with PBS and resuspended to $10x10^6$ cells/mL and labelled with 10 uM CFSE as described above. Cells were then washed three times with media and counted and resuspended to $1x10^6$ cells/mL. 2 ug/mL of CD3 cross-linking antibody was added to the cells and the mixture was incubated at 37°C for 30 minutes to allow binding of the antibody to Fc receptors on the surface of the P815 cells. $1x10^5$ cells were then plated per well in a 6 well culture dish. Pre-activated T cells from wild-type or *Rip3*$^{-/-}$ mice were collected, washed with PBS, and resuspended to $10x10^6$ cells/mL. Serial dilution was carried out to generate various effector T cell to target P815 cell ratios and the mixture was co-incubated overnight. The next day, cells were stained to assess viability, T cell activation, and secretion of IFN-gamma. Samples were analyzed by flow cytometry.

Adoptive transfer
T cells from 6-12 weeks old wild-type or *Rip3*$^{-/-}$ mice were harvested and purified from the spleen and lymph nodes by CD3 enrichment column. Cells were stimulated for 3 days with 2 µg/mL CD3 antibody, collected and washed three times with PBS and resuspended to $2x10^7$ cells/mL in sterile PBS. 6-12 week old CD45.1 B6 mice were used as recipients for intravenous transfer of the activated T cells. They were gently exposed to a heat lamp for 5-10 minutes prior to injection to dilate the blood vessel. 100 µL of T cell suspension was injected by tail vein per mouse. After recovery for 2-3 days, the recipient mice were challenged with MCA-303 tumor cells and growth of the tumors was measured. Alternatively, mice were first injected with tumors cells 5-7 days before adoptive transfer of T cells. Tumors were allowed to grow to about 10-50 mm^3 before transfer. In either case, mice were monitored daily and euthanized upon reaching endpoint as defined above.

Cell lines

MCA-303, B16 GM-CSF, and MC-38 cells were kind gifts obtained from David Raulet's lab and cultured in complete DMEM with 5-10% FBS. P815 cells were obtained from ATCC. T cells were grown in complete RPMI with 10% FBS for proliferation assays and adoptive transfers. However, for overnight incubations, T cells were kept in collection media with RPMI base supplemented with 5% serum.

Results

As has been previously published by others, when we first examined the RIP3 knockout mice, we observed no gross defects in physiology or in immune compartments[68]. Wild-type and knockout mice had comparable proportions of T and B cells in their spleen and lymph nodes (data not shown), suggesting homeostatic maintenance of T cells in the periphery is unaffected by ablation of RIP3. Thus we first aimed to determine what role RIP3 played in regulating the activation of naïve T cells. We performed an *in vitro* proliferation assay over the course of 144 hours to track activation and growth of T cells from *Rip3*$^{-/-}$ mice (**Fig 1.1**). Previously, we have shown that addition of nec-1 to CD3/CD28 cross-linking stimulation leads to increased number of CD8+ T cells at late time points[6], suggesting that TCR ligation may trigger downstream activation of necroptosis in this setting. Indeed, we saw that in T cells lacking RIP3 cell growth was enhanced at 120 hours and beyond post activation but unchanged at prior time points, which coincides with the onset of cell death in this assay (**Fig 1.1A**). This effect is much more pronounced in the CD8 compared to the CD4 compartment, with the rescue in CD8 T cells accounting for the majority of the difference between knockout and heterozygous controls.

Next we sought to examine the effect of inhibiting necroptosis on activation of T cells by assaying for the expression of various markers upregulated post-TCR ligation. Whereas we did not observe differences in the expression of early activation markers such as CD69 and CTLA-4 (**Fig 1.1B** and data not shown), we were able to initially find a reduction of PD-1 expression in late activation (**Fig 1.1C**). This decrease, however, was inconsistent through multiple repeats. In addition, we did not see any changes in CD44 (**Fig 1.1D**), CD62L, CD25, or FoxP3 expression (data not shown).

To verify the induction of necroptosis, we collected lysates at various time points after T cell activation and performed a native blot for RIP3 expression (**Fig 1.1E**). RIP3 forms large amyloid-like chains when it is phosphorylated and active which can be visualized under non-denaturing conditions[88]. Indeed, we detected high levels of 150 kDa and above species that were comparable to control L929 lysate in samples from the later time points, coinciding with the onset of contraction. As expected, we did not see appreciable levels of these bands in the *Rip3*$^{-/-}$ samples.

To determine whether the cause of the increased growth is due to enhanced proliferation due to an unknown function of RIP3 possibly in modulating cell growth, we CFSE labelled activated T cells to track their divisions over time (**Fig 1.2A**). We found no differences between the control and knockout T cells in frequency or number of divisions, suggesting the rescue we observed is not due to accelerated proliferation. In addition, we were able to mimic the rescue effect of knocking out RIP3 by using Nec-1s, a Nec-1 variant which is more specific for the RIP1 kinase activity. This again indicated that inhibition of RIP1-RIP3 dependent necroptosis downstream of TCR activation contributes to the increased numbers of T cells (**Fig 1.2B**).

Although we were unable to detect significant changes in the expression of activation markers on *Rip3*$^{-/-}$ T cells, we were nonetheless curious whether inhibition of necroptosis has any impact on T cell function. Particularly, since CD8 T cells exhibited far greater sensitivity to RIP3 deletion compared to CD4 T cells, we tested the cytotoxic activity of *Rip3*$^{-/-}$ T cells post-activation in a redirected lysis assay (**Fig 1.2C**). In this assay, T cells were co-incubated overnight with P815 mastocytoma cells, which bear Fc receptors on their surface. P815 cells were also pre-conjugated with α-CD3 and labelled with CFSE. Surface bound α-CD3 acts to recruit and activate CD8 T cells to lyse the target cells (P815), which can be visualized by loss of CFSE. To our surprise, we noted a consistent increase in target cell lysis by *Rip3*$^{-/-}$ T cells compared to control (6.25:1 and 12.5:1 target/effector ratios in **Fig. 1.2D** top panel, and lower ratios in bottom panel). Consistent with this, we also observed elevation in levels of IFN-γ in *Rip3*$^{-/-}$ CD8 T cells co-incubated with anti-CD3 coated P815 cells (**Fig. 1.2E**). A similar finding was also seen with wild-type T cells in the presence of Nec-1s (**Fig 1.2E**). As controls, CD4 T cells didn't show any cytotoxicity as expected. Independent repeats with lower effector/target ratios revealed similar trends in target cell loss and increased IFN-γ levels in effector RIP3-deficient CD8 T cells.

The physiological role of RIP3 in T cell function has thus far been limited to the context of viral infections or tissue injury. We were interested in exploring if the enhanced survival and cytotoxic activity we observed in *Rip3*$^{-/-}$ T cells may play a role in other processes, such as tumor control by CTLs. We injected 6-12 week old RIP3 knockout mice subcutaneously with a mildly immunogenic tumor cell line, MCA-303 (**Fig 1.3**). We observed slower tumor growth in the *Rip3*$^{-/-}$ mice compared to control as well as smaller tumor volumes overall, with some mice able to maintain a constant tumor size through the course of the experiment (**Fig 1.3A**). The delayed tumor growth corresponded to increased survival of *Rip3*$^{-/-}$ mice post-challenge, with some animals surviving for up to two weeks longer than control littermates (data not shown). When we examined the immune populations in tumor bearing mice by flow cytometry, we observed no differences in myeloid populations such as inflammatory monocytes and granulocytes between control and knockout mice in the spleen, draining and non-draining lymph nodes, or tumors (**Fig 1.3B**).

While we observed little to no difference in activation of the T cell populations in the spleen or lymph nodes of tumor bearing mice, we did find a slight decrease in PD-1 expression on CTLs in the tumor infiltrating lymphocytes, which corroborates our *in vitro* proliferation assay data (**Fig 1.3C, D**). Furthermore, we noticed reduced FoxP3 expression in the TILs as well as improved CD8 effector to Treg ratios, which correlate with our findings of reduced tumor growth and enhanced CTL activation (**Fig 1.3E, F**).

However, the *Rip3*$^{-/-}$ mice we used are whole animal knockouts and therefore we cannot definitely conclude the tumor suppression phenotype is due solely to enhanced survival and function of the CTLs or of immune populations. Thus we next adoptively transferred control or *Rip3*$^{-/-}$ T cells to wild-type CD45.1 B6 mice, which were used to differentiate between transferred and host T cells, as *Rip3*$^{-/-}$ mice are on the CD45.2 background. In this model, we were able to replicate the same enhanced tumor control phenotype we observed previously in the *Rip3*$^{-/-}$ animals. We saw both tumor burden and enhanced survival of the recipients across multiple independent repeats (**Fig 1.3G, H**). We adoptively transferred approximately three million activated T cells in these experiments because we reasoned we needed a relatively large pool of T cells to ensure recognition of the tumor antigen since we are not using a TCR transgenic model and the T cells had to be first properly activated for CD8 to differentiate into

effectors and for protection from necroptosis by RIP3 deficiency. Although we did not monitor the survival of these T cells *in vivo*, *in vitro* proliferation assays conducted parallel to the adoptive transfers did show the improved CD8 survival phenotype we observed in previous trials (data not shown). We also initially attempted to measure the tumor sizes in these experiments; however, most of the mice transferred with *Rip3*$^{-/-}$ T cells that were protected against tumor challenge did not develop tumors within the 30 day time frame of monitoring, which mirrors the stagnant tumor growth we observed in the *Rip3*$^{-/-}$ mice originally. We examined the TILs by flow cytometry. Curiously, we did not observe a significant difference in the CD8 to Treg ratio in the tumor but about a twofold increase ($p<0.05$) in the draining lymph nodes (data not shown). This data thus suggests that *Rip3*$^{-/-}$ CTLs are important for mediating tumor control. We also assessed whether we can replicate the phenotype by treating the mice with Nec-1s. We injected Nec-1s at previously published dosage for adult B6 mice (~1.5 μg/mg of body weight) every two days at the site of tumor injection, starting two days prior to challenge, until endpoint. However, we did not observe any differences in the treated and untreated groups, possibly due to confounding effects of Nec-1s on the tumor or other populations in the tumor microenvironment (data not shown).

Finally, we wanted to determine if *Rip3*$^{-/-}$ T cells are able to protect against prior tumor challenge. Therefore, we first injected CD45.1 mice with $5x10^4$ MCA-303 tumor cells, allowed the tumor to grow to a measurable size (~50 mm^3), and then transferred $1x10^6$ activated *Rip3*$^{-/-}$ T cells. Because MCA-303 tumors tend to ulcerate, even at low tumor volumes, we injected only mice that displayed no visible signs of ulceration with T cells. Although the effect we saw was not as dramatic, we were able to detect some degree of protection by the *Rip3*$^{-/-}$ T cells post tumor challenge (**Fig 1.4A**). While one mouse from the *Rip3*$^{-/-}$ transferred group in each repeat of the experiment was able to completely reject the tumor or arrest its growth, the majority of the recipients displayed delayed growth compared to the heterozygous wild-type transferred group. However, the rate of ulceration was similar between both groups and thus we euthanized the mice at similar time points. When we analyzed the TILs by flow, we observed elevated activation of CTLs from *Rip3*$^{-/-}$ donors as demonstrated by higher expression of CD44 as well as enhanced function of these cells as reflected by increased IFN-γ secretion upon stimulation with tumor lysate (**Fig 1.4B, C**).

Due to the attenuated protection afforded by *Rip3*$^{-/-}$ T cells against prior MCA-303 tumor challenge that varies somewhat in different experiments (Fig. 1.4A, F), we questioned if combining *Rip3*$^{-/-}$ adoptive transfer with other immunotherapies may strengthen the antitumor effect. We injected CD45.1 recipients with MC-38 cells, which have been shown to express high levels of PD-L1 and are recalcitrant to *Rip3*$^{-/-}$ transfer treatment. Three days later, we adoptively transferred activated T cells from *Rip3*$^{-/-}$ mice and their littermate controls. In one group of mice, we also injected anti-CTLA-4 antibodies on the right flank of recipients. We repeated the antibody administration two more times every two days and monitored the growth of the tumors. The antibody alone has been reported to confer some protection against MC-38 tumor[89]. While the tumor volume was similar between *Rip3*$^{-/-}$ and *Rip3*$^{+/-}$ samples in the presence of anti-CTLA-4, significantly more mice survived in the *Rip3*$^{-/-}$/anti-CTLA-4 group when compared to the *Rip3*$^{+/-}$/anti-CTLA-4 group (Fig 1.4D, E). Furthermore, three out of six mice receiving *Rip3*$^{-/-}$ /anti-CTLA-4 remained tumor free after 30 days compared to just one in the *Rip3*$^{+/-}$/anti-CTLA-4 group. We extended these findings to the MCA-303 cell line and observed that combination therapy resulted in a similar strong antitumor response against prior challenge across two repeats (**Fig 1.4F**). However, in the MCA-303 experiments, we did not include an antibody only or

Rip3$^{+/-}$/anti-CTLA-4 group and thus can't exclude the possibility the antibody may confer strong protection on its own. We are currently performing trials to resolve this issue.

To further assess the contribution of T cells to this phenotype, we adoptively transferred T cells from *Rip3*$^{-/-}$ T cells to *Rag2*$^{-/-}$ recipients and then challenged the mice with tumors. Surprisingly, we detected no differences in tumor growth or host survival in three independent trials between *Rag2*$^{-/-}$ recipients transferred with wild-type or *Rip3*$^{-/-}$ T cells (representative data from one trial shown in **Fig 1.5A and B**). When we examined the TILs by flow cytometry, we observed no noticeable differences in any of the markers we assayed above. Since *Rag2*$^{-/-}$ mice also lack B cells and this difference may account for the discrepancy in phenotype, we co-transferred both B and T cells from *Rip3*$^{-/-}$ animals to recipients. However, we still did not detect a notable difference in tumor size either in these experiments (**Fig 1.5C and D**). These data might suggest that the anti-tumor effects of *Rip3*$^{-/-}$ T cells may depend on host T cells. Alternatively, the lack of RAG2 in *Rag2*$^{-/-}$ recipients may have altered host environment in a way that doesn't allow reconstitution of anti-tumor immunity by adoptively transferring T cells.

Discussion

The relationship between cancer and the immune system has been increasingly appreciated in recent years[69,70]. A tug-of-war between the tumor, which employs a variety of mechanisms such as MHC downregulation and secretion of inhibitory cytokines to escape detection and deletion by the immune system, and adaptive immune cells, particularly T cells, and between the pro- and anti-tumor effects of immune populations themselves has tremendous consequences on tumor control. Inhibition of T cell function by tumors, through upregulation of inhibitory markers such as PD-L1, plays a crucial role in tumor immune evasion and blocking or reversing these pathways has been revealed to be invaluable in the clinic for treating certain types of cancer, such as melanomas and lymphomas, unamenable to conventional therapies[2,61]. These treatments also serve as new windows into helping us understand the complex regulation and function of T cell populations in a physiological setting and offer insights into the basic biology of T cell activation.

We show here that one such pathway that may regulate T cell function in a tumor setting is necroptosis, an alternate programmed cell death pathway normally triggered in the absence of apoptosis and downstream of infection or injury. Necroptosis plays an important role in the homeostasis and activation of a variety of immune cell types, such as macrophages and dendritic cells[71,72]. Due to this prior observation and our understanding of necroptosis, we examined the phenotype of T cells from mice lacking RIP3, an interacting partner of RIP1 in necroptosis. We demonstrated that, when RIP3 is ablated in T cells, they are able to survive and proliferate for much longer post-activation compared to their wild-type counterparts. This death seems to occur late in activation, starting from 72 hours and extending to 120 hours, as revealed by time course experiments. As RIP1 and RIP3 have been shown to be expressed early in T cell activation (within 48 hours), the delayed onset of cell death may reflect additional regulatory mechanisms that may prevent the activation of the kinase activity of either of the two proteins in the absence of further death inducing signals. This hypothesis is consistent with the kinetics of T cell activation, as activated T cells first rapidly expand then just as rapidly contract and therefore having RIP1 and RIP3 already expressed and available can greatly accelerate the contraction phase. We confirmed that the increased numbers of T cells were not due to enhanced proliferation as *Rip3*$^{-/-}$ T cells display no gross differences in rates of division as tracked by

CFSE staining, suggesting that the activated *Rip3*$^{-/-}$ T cells that accumulate have escaped from death by necroptosis. This hypothesis is further corroborated by the similarly elevated cell numbers observed when wild-type activated T cells are cultured in the presence of Nec-1s, a more specific RIP1 kinase inhibitor than Nec-1[65].

What the induction of necroptosis in dying activated T cells means is puzzling. Necroptosis is by nature a "messy" form of cell death involving membrane disruption and leakage of intracellular contents and can trigger a potent inflammatory response through release of DAMPs[17,73,74]. Consistent with this view, DC- or macrophage-specific FADD knockout mice suffer from systemic inflammation[75,76]. Interestingly, however, T-cell specific FADD deficient mice do not[6]. Thus, necroptotic T cells are possibly not immunogenic, for unknown reasons, or this pathway plays only a minor role in homeostatic maintenance of peripheral T cell populations and may only be activated in the context of TCR stimulation, such as in an infection. In either case, why T cells may undergo such a potentially inflammatory form of cell death during the contraction phase of the adaptive immune response, when their function is attenuated, is confounding and appears at first to be counterintuitive. One possibility is that necroptosis may cross-talk with other pathways in T cell activation to control T cell function. Expression of cFLIP isoforms, which is regulated by TCR signaling, may lead to inhibition of caspase-8 and render the cells susceptible to necroptosis[77,78]. Another possibility is that this process does not occur physiologically and that our *in vitro* stimulation introduces artificial conditions, such as poor nutrients and lack of additional cytokines in the culture medium, that cause the T cells to initiate an emergency shutdown response. However, the fact that *Rip3*$^{-/-}$ T cells can confer enhanced anti-tumor immunity suggests that they do have increased activities *in vivo*.

Indeed, in addition to their increased survival upon activation, *Rip3*$^{-/-}$ T cells displayed enhanced cytotoxic activity. They were able to kill a target tumor cell line at 2-3 times the efficiency of control T cells and secreted similarly higher levels of effector cytokines. This elevated functionality may reflect the greater proportions of CTLs that are rescued by necroptosis inhibition and suggests that these CTLs remain functional despite having persisted past the normal onset of contraction.

The functional rescue of these CTLs led us to test the contribution of necroptosis in a physiological setting. We observed a drastic reduction in tumor size and growth in *Rip3*$^{-/-}$ animals and increased expression of activation markers and elevated cytokine secretion, mirroring results from the *in vitro* proliferation and cytotoxicity assays. In adoptive transfer experiments, we saw similar levels of protection. Together, the data suggest that necroptosis may indeed play a role in regulating T cell activation in a physiological setting. However, in both the endogenous and adoptive transfer models, we did not detect any significant differences in the myeloid populations in the tumor or draining lymph nodes, suggesting that the rescue we see is chiefly due to the T cell compartment. Thus, inhibiting necroptosis in activated T cells may help rescue functional CTLs that otherwise may perish during the contraction phase of the immune response and that these CTLs can provide protection against tumor challenge.

In contrast to the effective antitumor protection we saw in these experiments, we observed weak responses when we implanted the tumor prior to adoptive transfer, suggesting that potentially multiple rounds of transfer or combination treatment with checkpoint blockade inhibitors to ameliorate tumor-mediated immune suppression may be required in this more clinically relevant setting to confer adequate protection. Indeed, when we carried out these combination therapies, we found that tumor growth was once more significantly reduced and that some mice remained tumor free. The strength of the protection was comparable to adoptive

transfer of *Rip3*$^{-/-}$ T cells before tumor challenge. Thus, rescuing both the survival – through inhibition of necroptosis – and function – through blocking inhibitory receptors – of CD8 effector T cells may be a synergistic strategy for antitumor treatment. However, as we have only so far shown modest protection in two tumor models with anti-CTLA-4 antibodies, testing of additional tumor cell lines and using anti-PD1 antibodies will be needed to determine whether this effect is broadly applicable. Finally, adoptively transferring T cells more than once might also increase the protective effects.

The interaction between the transferred and host T cells is unclear. Determining whether the tumor protection we observe is driven entirely by the *Rip3*$^{-/-}$ CD8 effectors or if cross-talk between these (or CD4) and host T cells is also important is interesting and we are currently performing CD8 only adoptive transfers to address this question. We are also tracking tumor specific T cells by tetramer staining in the MC-38 model and examining whether this population is expanded in the host upon transfer and if we can observe changes in their activation status as well as cytokine profile.

In summary, necroptosis appears to be able to be triggered downstream of TCR ligation and this pathway seems important for limiting the number of active CD8 T cells during the contraction phase of the immune response. RIP3 ablation can rescue these T cells and restore their function both *in vitro* and *in vivo*. This rescued population may offer protection against tumor growth, though the magnitude of the effect seems to be weakened when tumors are injected prior to transfer of *Rip3*$^{-/-}$ T cells. The elevated numbers of activated CD8 T cells in *Rip3*$^{-/-}$ mice appear to better control tumors through secretion of effector cytokines and a shift in the T cell populations in the tumor towards a CD8 and away from a Treg dominant response. Blocking T cell necroptosis for tumor treatment may therefore act in synergy with checkpoint blockade therapy to not only revert suppression of T cell function but also improve their survival and proliferation to generate a more potent immune response against the tumor. Understanding the control of T cell activation induced necroptosis may help to identify further targets for treatment and provide insights into the regulation of the antitumor adaptive immune response.

FIGURE LEGENDS
FIGURE 1.1

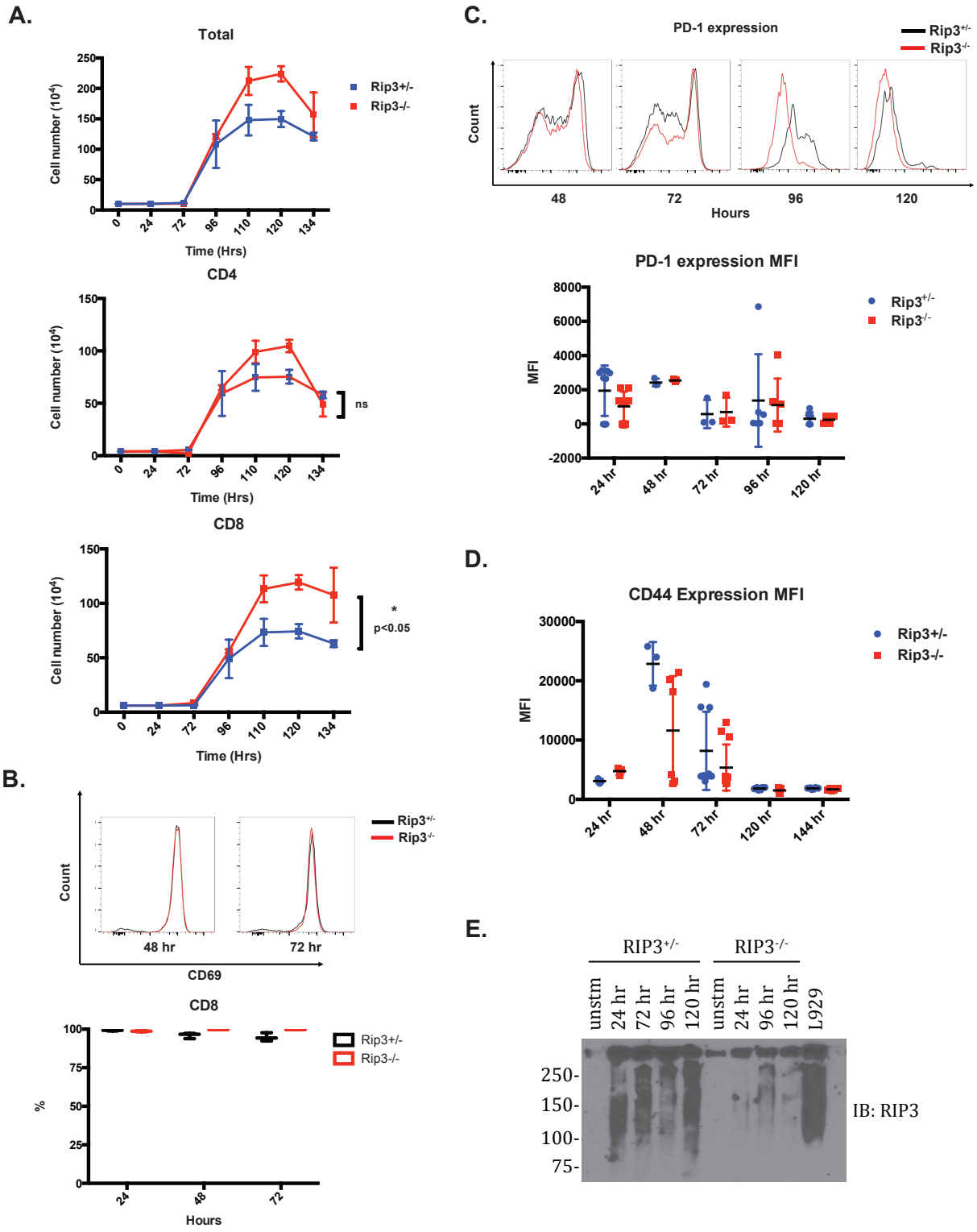

Figure 1.1 *Rip3*$^{-/-}$ T cells show enhanced survival upon activation. A) Proliferation of activated T cells from *Rip3*$^{-/-}$ or heterozygous littermates upon activation with CD3/CD28 cross-linking. T cells were purified by CD3 enrichment from spleen and lymph nodes of six to twelve week old mice and stimulated at a density of $1x10^6$ cells/mL with 2 μg/mL of plate-bound α-CD3/CD28 antibody. Live cell counts were collected from triplicate wells every 24 hours by Trypan blue staining, with total counts (top), CD4 (middle), and CD8 (bottom) shown. Data have been repeated at least five times with similar results. B) Early activation status of *Rip3*$^{-/-}$ T cells as measured by CD69 staining. T cells were collected 24, 48 or 72 hours post-activation and stained with CD69-FITC antibody then analyzed by flow cytometry. Top shows representative raw flow data and bottom shows compiled expression data expressed as a percentage of total CD8 population over five replicate experiments. C) and D) Late activation status of *Rip3*$^{-/-}$ T cells shown by PD-1 and CD44 expression. Activated T cells were collected and stained for PD-1 and CD44 for flow analysis at the time points indicated. C) top panel indicates representative raw flow data while C) bottom and D) shows compiled data from greater than three repeat experiments with each data point corresponding to one mouse. E) Activation and formation of high molecular weight species of RIP3 during late T cell activation revealed by native blot. Lysates from *Rip3*$^{+/-}$ or *Rip3*$^{-/-}$ purified T cells were collected at various time points after activation and equal amounts of protein were loaded onto a denaturing gel and immunoblotted for total RIP3 overnight.

FIGURE 1.2

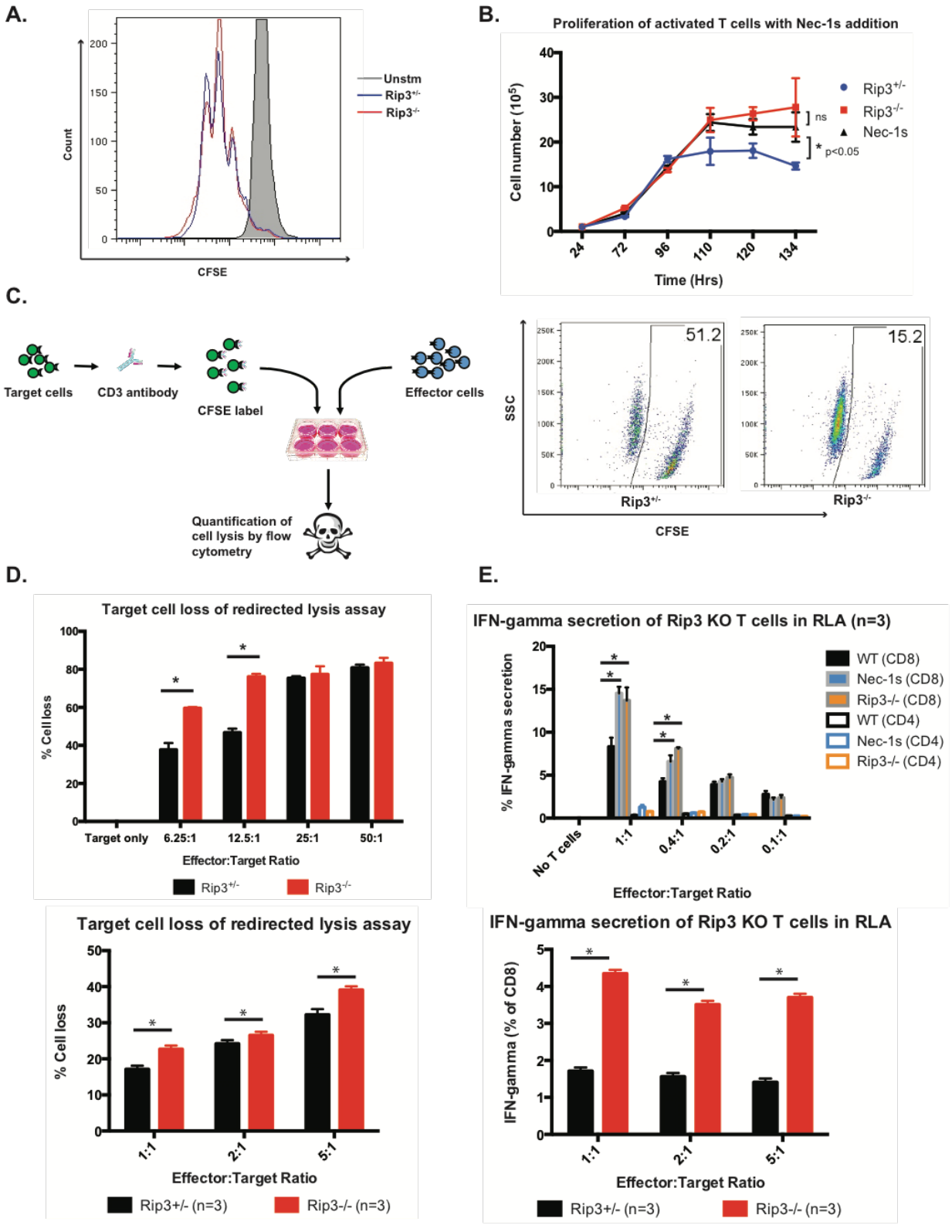
A.
Count
CFSE
Unstm
Rip3+/-
Rip3-/-
B.
Proliferation of activated T cells with Nec-1s addition
Cell number (10^5)
Time (Hrs)
Rip3+/-
Rip3-/-
Nec-1s
ns
* p<0.05
C.
Target cells
CD3 antibody
CFSE label
Effector cells
Quantification of cell lysis by flow cytometry
SSC
51.2
15.2
Rip3+/-
Rip3-/-
CFSE
D.
Target cell loss of redirected lysis assay
% Cell loss
Target only
6.25:1
12.5:1
25:1
50:1
Effector:Target Ratio
Rip3+/-
Rip3-/-
E.
IFN-gamma secretion of Rip3 KO T cells in RLA (n=3)
% IFN-gamma secretion
No T cells
1:1
0.4:1
0.2:1
0.1:1
Effector:Target Ratio
WT (CD8)
Nec-1s (CD8)
Rip3-/- (CD8)
WT (CD4)
Nec-1s (CD4)
Rip3-/- (CD4)
Target cell loss of redirected lysis assay
% Cell loss
1:1
2:1
5:1
Effector:Target Ratio
Rip3+/- (n=3)
Rip3-/- (n=3)
IFN-gamma secretion of Rip3 KO T cells in RLA
IFN-gamma (% of CD8)
1:1
2:1
5:1
Effector:Target Ratio
Rip3+/- (n=3)
Rip3-/- (n=3)

Fig 1.2 Enhanced cytotoxic activity of *Rip3*$^{-/-}$ T cells. A) CFSE tracking of *Rip3*$^{-/-}$ T cells post-activation. CD3 column enriched T cells from six to twelve weeks *Rip3*$^{+/-}$ or *Rip3*$^{-/-}$ mice were labelled with CFSE and activated with CD3/CD28 antibody stimulation for seven days. T cells were collected at end of time course and analyzed by FACS. Representative data shown of three repeat experiments. B) Comparison of rescue from necroptosis upon Nec-1s addition with RIP3 ablation in activated T cells. Purified T cells were activated with plate-bound CD3/CD28 antibody for seven days. Nec-1s (30 μM) was added at the start of culture and renewed every 24 hours. Live cells were counted each day by Trypan blue staining and proliferation was plotted. Data have been repeated at least three times with similar results. C) Schematic of redirected lysis assay and representative results. Briefly, P815 target cells were conjugated with α-CD3 antibody and labelled with CFSE. Activated T cells from *Rip3*$^{+/-}$ and *Rip3*$^{-/-}$ mice were co-incubated with target T cells overnight and flow analysis was performed the following day to measure CFSE loss from dying target cells. Right panel, representative raw flow data from effector cells added to target cells at a 12.5:1 ratio. D) Specific lysis of target P815 cells by control and RIP3 knockout T cells in a redirected lysis assay. Results are from two repeats (top) and an additional independent repeat with lower effector/target ratio (bottom). E) Secretion of IFN-γ by CD4 and CD8 T cells in lysis assay as measured by flow cytometry in a redirected lysis assay. After co-incubation of target P815 cells with T cells overnight, IFN-γ expression of T cells was measured by intracellular staining and fixing with BD Cytofix kit and analyzed by FACS. Results compiled from three independent experiments (top) and from another independent experiment with higher effector/target ratios (bottom). *$p<0.01$

FIGURE 1.3

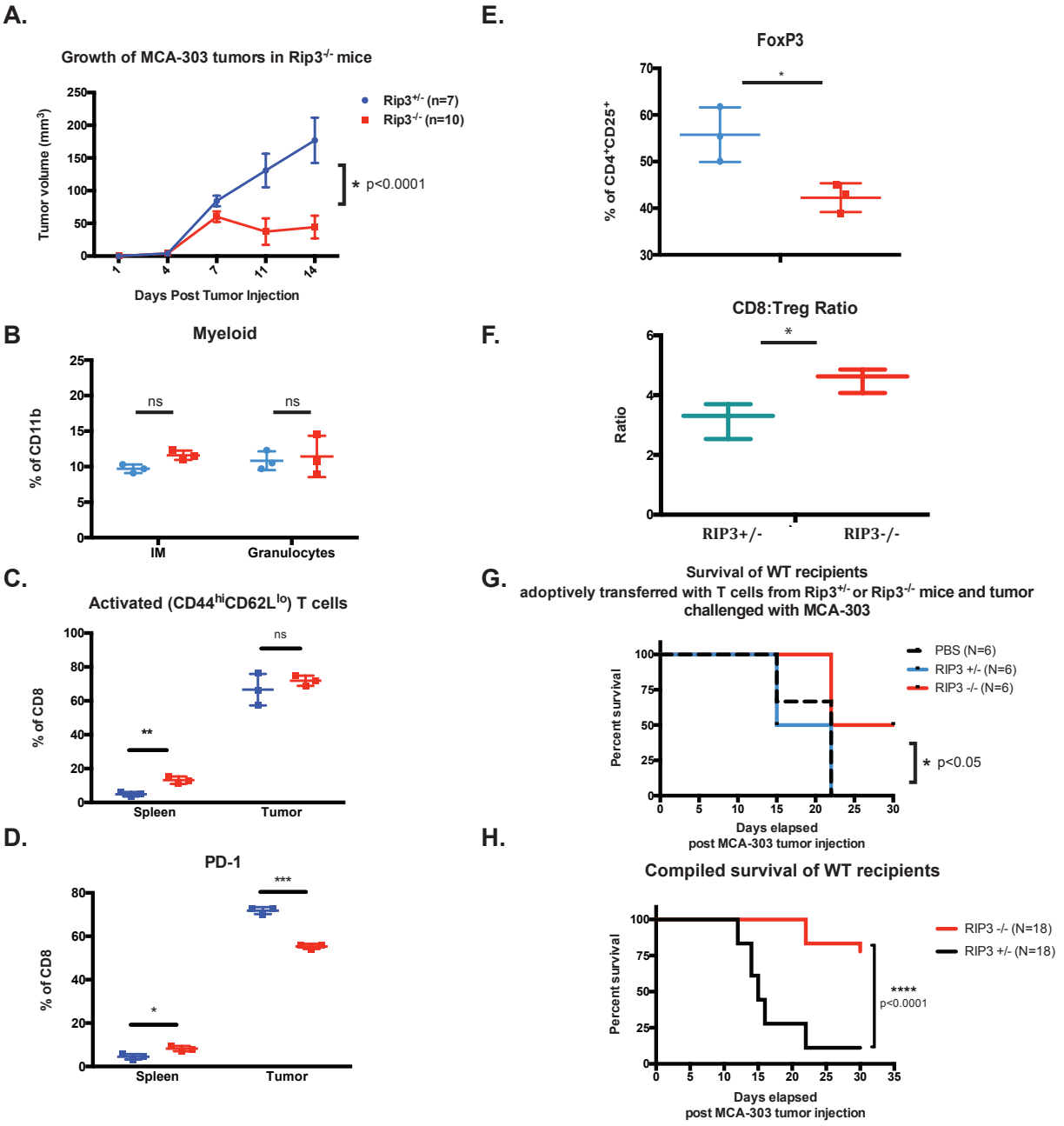
A.
Growth of MCA-303 tumors in Rip3-/- mice
Tumor volume (mm3)
Days Post Tumor Injection
Rip3+/- (n=7)
Rip3-/- (n=10)
* p<0.0001
B
Myeloid
% of CD11b
ns
ns
IM
Granulocytes
C.
Activated (CD44hiCD62Llo) T cells
% of CD8
**
ns
Spleen
Tumor
D.
PD-1
% of CD8
*
***
Spleen
Tumor
E.
FoxP3
% of CD4+CD25+
*
F.
CD8:Treg Ratio
Ratio
*
RIP3+/-
RIP3-/-
G.
Survival of WT recipients
adoptively transferred with T cells from Rip3+/- or Rip3-/- mice and tumor challenged with MCA-303
Percent survival
Days elapsed
post MCA-303 tumor injection
PBS (N=6)
RIP3 +/- (N=6)
RIP3 -/- (N=6)
* p<0.05
H.
Compiled survival of WT recipients
Percent survival
Days elapsed
post MCA-303 tumor injection
RIP3 -/- (N=18)
RIP3 +/- (N=18)
****
p<0.0001

Figure 1.3 *Rip3*$^{-/-}$ mice better control tumors due to enhanced CTL survival and function. A) Growth of MCA-303 tumors. MCA-303 cells were injected subcutaneously and growth was measured every two to three days. Tumor volume was calculated with the modified ellipse formula *½(length x width^2)*. Mice were euthanized upon tumor ulceration or approaching a volume of 1 cm^3. Data were repeated twice with similar results. B) – F) Spleen and lymph nodes were collected from tumor bearing mice upon reaching experimental endpoint and processed into single cell suspensions for flow analysis. B) Proportions of inflammatory monocytes and granulocytes in TILs. C) CD44 and CD62L expression on CD8 T cells in spleen and tumor. D) PD-1 expression on CD8 T cells in spleen and tumor infiltrating lymphocyte populations. E) FoxP3 expression of CD4$^+$CD25$^+$ T cells in TIL compartment. F) CD8 effector to CD4$^+$CD25$^+$Foxp3$^+$ Treg ratios calculated as percentage of CD8 divided by percentage of Treg in the TILs. E) Proportions of inflammatory monocytes and granulocytes in TILs. G) Survival of CD45.1 recipients post adoptive transfer with *Rip3*$^{-/-}$ T cells upon tumor challenge. CD45.1 recipients were injected intravenously through the tail with 2-3x10^6 *Rip3*$^{+/-}$ or *Rip3*$^{-/-}$ T cells. The T cells had previously been purified from six to twelve week old littermates and activated with plate-bound CD3/CD28 antibody for 2-3 days. After allowing CD45.1 recipients to recover for 2-3 days, MCA-303 cells were injected subcutaneously and mouse survival was monitored until tumors reached endpoint or up to one month. H) Compiled survival curves of adoptive transfer trials from four individual experiments.

FIGURE 1.4

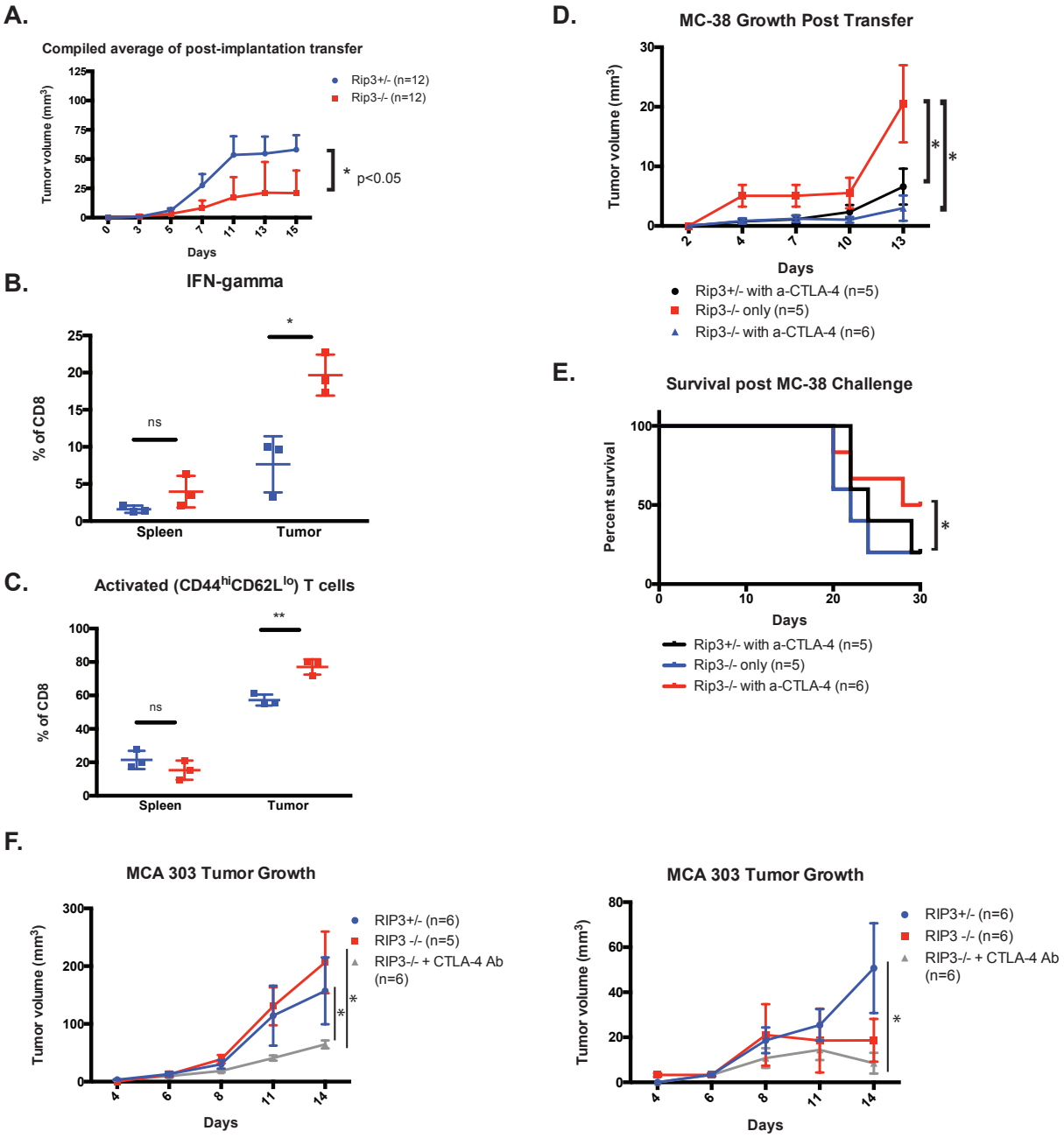
A.
Compiled average of post-implantation transfer
Tumor volume (mm3)
Days
Rip3+/- (n=12)
Rip3-/- (n=12)
* p<0.05
B.
IFN-gamma
% of CD8
ns
*
Spleen
Tumor
C.
Activated (CD44hiCD62Llo) T cells
% of CD8
ns
**
Spleen
Tumor
D.
MC-38 Growth Post Transfer
Tumor volume (mm3)
Days
Rip3+/- with a-CTLA-4 (n=5)
Rip3-/- only (n=5)
Rip3-/- with a-CTLA-4 (n=6)
E.
Survival post MC-38 Challenge
Percent survival
Days
Rip3+/- with a-CTLA-4 (n=5)
Rip3-/- only (n=5)
Rip3-/- with a-CTLA-4 (n=6)
F.
MCA 303 Tumor Growth
Tumor volume (mm3)
Days
RIP3+/- (n=6)
RIP3 -/- (n=5)
RIP3-/- + CTLA-4 Ab (n=6)
MCA 303 Tumor Growth
Tumor volume (mm3)
Days
RIP3+/- (n=6)
RIP3 -/- (n=6)
RIP3-/- + CTLA-4 Ab (n=6)

Figure 1.4 Adoptive transfer of *Rip3*$^{-/-}$ T cells in conjunction with anti-CTLA-4 blockade post-tumor challenge is able to effectively protect against tumor growth. A) Growth of MCA-303 tumors in CD45.1 hosts upon transfer of *Rip3*$^{-/-}$ T cells compiled from two individual experiments. MCA-303 tumor cells were injected subcutaneously on the right flank of CD45.1 mice and allowed to grow to until reaching a size of around 50 mm^3. $1x10^6$ purified, activated *Rip3*$^{+/-}$ or *Rip3*$^{-/-}$ T cells were then transferred IV into the tail vein and tumor growth was measured post-treatment until tumors reached endpoint. B) IFN-γ secretion of CD8 T cells in spleen and TIL of recipient mice. Spleen, lymph nodes, and tumors were collected and dissociated as described above and stained intracellularly for IFN-γ expression with BD Cytofix kit. Before staining, T cells from the spleen or the TIL were first re-activated with plate-bound CD3/CD28 antibody overnight in the presence of Golgi inhibitors. Each data point corresponds to one mouse and the experiment has been repeated twice. C) CD44 and CD62L expression of CD8 T cells from the same experiments in B). D) Growth of MC-38 tumors in CD45.1 hosts after combination therapy with *Rip3*$^{-/-}$ T cell adoptive transfer and anti-CTLA-4 blockade. $1x10^5$ MC-38 cells were injected subcutaneously on the right flank of host mice and three days later T cells were transferred IV as described above. 100 μg of CTLA-4 antibody (UC10-4F10-11) were injected IP at the same time and subsequently administered two additonal times, 50 μg each time, every two days. Tumor growth was tracked until endpoint. E) Survival of MC-38 tumor bearing mice after combination therapy. F) Growth of MCA-303 tumors upon treatment with post-implantation combination therapy from two individual repeats (left and right). MCA-303 tumors were injected on the right flank of CD45.1 mice and adoptive transfer in conjunction with CTLA-4 antibody administration were carried out as described above. Tumor growth was tracked until endpoint.

FIGURE 1.5

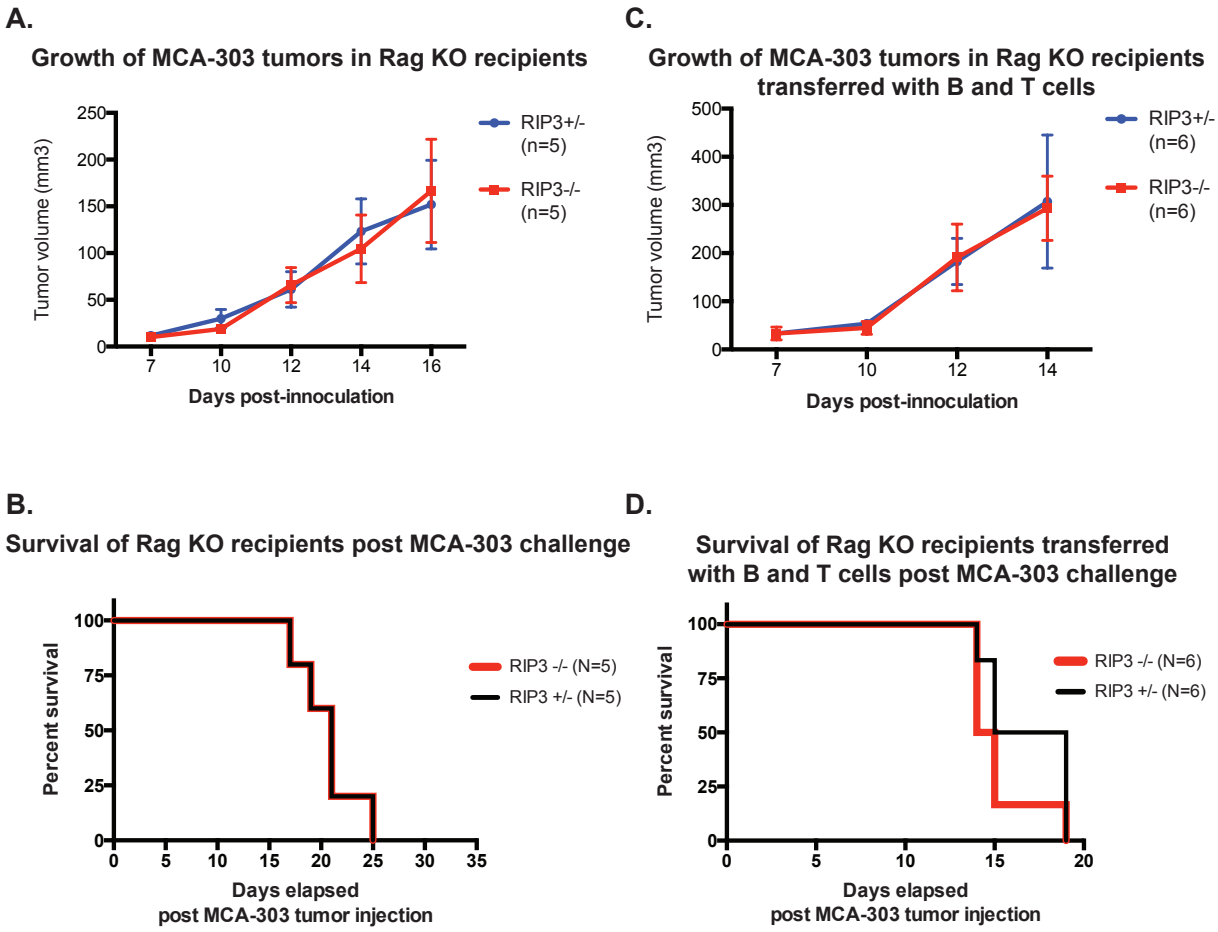
A.
Growth of MCA-303 tumors in Rag KO recipients
Tumor volume (mm3)
250
200
150
100
50
0
7
10
12
14
16
Days post-innoculation
RIP3+/- (n=5)
RIP3-/- (n=5)
C.
Growth of MCA-303 tumors in Rag KO recipients transferred with B and T cells
Tumor volume (mm3)
500
400
300
200
100
0
7
10
12
14
Days post-innoculation
RIP3+/- (n=6)
RIP3-/- (n=6)
B.
Survival of Rag KO recipients post MCA-303 challenge
Percent survival
100
75
50
25
0
0
5
10
15
20
25
30
35
Days elapsed post MCA-303 tumor injection
RIP3 -/- (N=5)
RIP3 +/- (N=5)
D.
Survival of Rag KO recipients transferred with B and T cells post MCA-303 challenge
Percent survival
100
75
50
25
0
0
5
10
15
20
Days elapsed post MCA-303 tumor injection
RIP3 -/- (N=6)
RIP3 +/- (N=6)

Fig 1.5 Adoptive transfer of *Rip3*$^{-/-}$ T cells into Rag deficient recipients does not protect against tumor challenge. A) and B) Growth and survival respectively of Rag KO recipients upon MCA-303 tumor injection post-transfer of *Rip3*$^{-/-}$ T cells. T cells from RIP3 knockout mice were purified and activated with CD3/CD28 stimulation for 72 hours, then washed, and $3x10^6$ cells was injected IV through the tail vein into Rag KO recipients. Mice were allowed to recover for three days before subcutaneous injection with $1x10^5$ MCA-303 tumor cells. Growth and survival was measured every two days. C) and D) Growth and survival of Rag KO mice upon transfer of B and T cells from *Rip3*$^{-/-}$ mice. B and T cells were collected through negative enrichment by magnetic bead purification and stimulated and injected as per above. Tumor growth and animal survival was measured.

Chapter 2: Designing a modified tandem affinity (moTAP) pulldown approach to identifying interacting partners of RIP3 in T cell activation induced necroptosis

Introduction

While the biochemical engine – RIP3 and MLKL phosphorylation and induction – that drives necroptosis remains mostly constant downstream of necroptosis' various activating pathways, the key interacting molecules that partner with and regulate RIP3 and MLKL can vary greatly[79,80]. For example, the death domain containing adaptor molecules FADD, TRADD, and MyD88 can be recruited to Fas, TNFR1, and TLRs respectively in response to infection or injury to trigger necroptosis[81]. In addition, TRIF is important for linking TLR3/4 signaling to necroptosis in BMDMs via the RHIM domain it shares with RIP1/3[31]. Given the complexity of necroptotic signaling and the difficulty of determining the timing and nature of the upstream signals that may trigger the pathway in activated T cells, we aimed to utilize a bait approach to identify the important molecules involved in activation induced necroptosis in T cells to help us better understand the regulation of this process.

Previously, RIP1 and RIP3 have been shown to associate with each other upon T cell activation due to an ubiquitination event at Lys5 on RIP3 and that the ubiquitin modifying enzyme A20 plays a negative, protective role in this process, preventing T cells from undergoing necroptosis[40]. Whether A20 acts in concert with other proteins in this regulatory function, what upstream signals recruit these complexes and how these signals are transduced directly or indirectly, potentially through the action of transcription factors, from the TCR, and what other factors may be involved to turn on RIP3 during induction of necroptosis are all still unclear. Perhaps one of the most apparent mechanisms for triggering necroptosis in activated T cells is through the TNFR family of death receptors, the ligands for some of which - such as FasL - are upregulated upon TCR induction through some of the cytokines, including IL-2 acting through Stat5, that are produced during this very process, thus serving as an elegant negative feedback loop to check T cell proliferation and limit the immune response[82]. However, unpublished data from our lab appears to show that neither Fas nor TNFR seems to play a role in this process as blocking antibodies to these receptors failed to rescue necroptosis in FADD deficient T cells while addition of Nec-1 rescues the death almost completely.

An alternate possibility for the source of the inducing signal is that it derives from intracellular factors, such as transcriptional programs activated by the TCR or metabolic shifts that occur when T cells transition from a quiescent to a proliferative state. Recent evidence from dendritic cells may support the latter notion, as DCs undergoing aerobic glycolysis appear more sensitive to zVAD induced necroptosis and this propensity to undergo necroptosis can be altered by changing the metabolic program through the addition of 2DG to the culture[83,84]. As activated T cells also adopt aerobic glycolysis to sustain their rapid expansion and may enter a state of hypoxia, which has been shown to initiate necroptosis, at least in cancer cell lines, an entirely different signaling origin may be responsible for the activation induced cell death of T cells[85]. Thus, since we are not sure of the exact nature of the upstream signals that can lead to T cell necroptosis but have in our possession evidence that RIP3 may be critical for this process, we generated a modified tandem affinity (moTAP) tagged RIP3 construct to purify the RIP3 associating complex in T cells upon necroptosis induction and analyze its components by mass spectrometry. This moTAP approach has been previously optimized to successfully identify

members of the ubiquitin interaction complex that modifies RIP1 downstream of TNFR ligation in mammalian cells and is a powerful tool because of its high specificity[86].

Materials and Methods

Plasmids and cloning
The modified tandem affinity tag consists of 2x FLAG and 2x Strep tags separated by a PreScission protease cleavage site. The tag was added to the N-terminus of human RIP3 (vector containing human RIP3 cDNA was a kind gift from Francis Chan) and mouse RIP3 (cDNA isolated from activated B6 T cells). Primer used for introduction of the tag is as follows: 5'-ATATGCTAGCGCCGCCGCCATGGACTACAAAGACGATGACGACAAGGACTACAAAGACGATGACGACAAGCTGGAAGTGCTGTTTCAGGGCCCGAAGTGGTCACATCCACAATTCGAGAAGTGGTCACATCCACAATTCGAGAAGTCGTGCGTCAAGTTATGG-3' and the tagged RIP3 was amplified and cloned into various vectors, including pCI, pcDNA3.1, pMSCV-PIG, pMSCV-neo, by restriction enzyme digest as well as Gibson ligation.

Mice
Twelve week old B6 mice were used as the source of T cells for transductions. T cells were purified by CD3 enrichment column from spleen and lymph nodes, activated by 4 μg/mL of CD3 and CD28 antibodies in the presence of 20 units of IL-2 for up to two weeks, then harvested and lysed for analysis of protein expression and co-immunoprecipitations.

Transfection of NIH-3T3 cells
NIH-3T3 N cells were seeded at a density of $2x10^5$ cells/mL day prior to transfection in 10 cm^2 or 6 well culture dishes. Five to ten μg of Maxiprep plasmid DNA containing moTAP RIP3 (pCI or pcDNA3.1) was used for transfection with Lipofectamine 2000 (Invitrogen) per manufacturer protocol. Four hours post transfection, media was refreshed and cells were treated with DMSO mock or 10-100 ng/mL of recombinant mouse TNFα (Biolegend) and 10-20 μM of zVAD (Sigma). Cells were harvested and lysed 24-48 hours post-treatment for immunoprecipitation and Western blot.

Transduction of L929 cells
Phoenix (Px) cells were a kind gift from from Garry Nolan. Px cells were used for retrovirus generation and seeded at $5x10^6$ cells per 10 cm^2 plate day prior to transfection. 10 μg of pMSCV-PIG or neo2.2 moTAP RIP3 was transfected by Lipofectamine 2000 along with 3μg of VSVG and 1.5 μg Nolan helper plasmid (also from the Nolan lab). Supernatant containing virus was collected and purified through a 0.2 μM syringe filter (Nalgene) 48-72 hours post Px cell transfection. L929 fibrosacorma cells were seeded at approximately $2x10^5$ cells/mL day before transduction. L929 cells were infected at a 1:1 ratio of viral media to cell culture media. Polybrene (Millipore) was added at 10 ug/mL to enhance the efficiency of the transduction. Cells were centrifuged for 1 hour at 1000 g at room temperature then cultured for up to 72 hours in fresh medium. Expression of GFP was monitored daily by microscopy or flow cytometry and cells were harvested for WB and co-IP.

Transduction of T cells

Virus was generated and T cells were purified and activated as above. Prior to transduction of T cells, virus was concentrated by spinning at 30,000 g at 4°C for 2 hr. Concentrated virus was added to activated T cells at a ratio of 100 μL of virus per 1 mL of culture and the cells were spun and infected as above. T cells were monitored daily for GFP expression, viability, and activation marker expression by flow cytometry and harvested 5-7 days post transduction for Western blot analysis.

Western blotting

RIP1 (BD), RIP3 (ProSci), FLAG (Sigma), Strep (Abcam), and actin (Sigma) were used at manufacturer specified concentrations. Membranes were incubated with 4% BSA for 30 min and primary was then added for 2 hours at room temperature or overnight at 4°C. Secondary (mouse IgG2a, mouse IgG1, rabbit polyclonal HRP from ThermoFisher) was added for 1 hour at 1:10,000 or 1:20,000 dilution. Bands were visualized by SuperSignal Chemiluminescent kit (ThermoFisher).

Co-Immunoprecipitation of moTAP RIP3 complexes

Cells were lysed for 30 minutes on ice with standard 1% NP-40 lysis buffer (50 mM Tris pH 7.8, 150 mM NaCl, 1% NP-40, protease inhibitor cocktail (Sigma)) and supernatant was cleared by centrifugation for 10 min at 15,000 g at 4°C. Protein was quantitated with BCA kit (Bio-Rad) per manufacturer instructions and protein complexes were immunoprecipitated with 1 ug of specified antibody per 1 mg of protein. Lysate was incubated overnight with pulldown antibody and 20 μL of protein A/G agarose beads (Pierce). Tagged RIP3 construct was eluted either by 3x FLAG peptide competition (Sigma) or cleavage with PreScission protease (GE) at a titration for 30 minutes to overnight at 4°C. The eluate was subjected to a second round of purification by pulldown with 20 μL of Streptavidin sepharose beads (GE) and subsequent column elution by competition with desthiobiotin (IBA) for 30 minutes. Samples were boiled and denatured with 4x SDS and loaded onto a 10% SDS-PAGE gel for Western blot analysis.

Results

We generated a modified tandem affinity tagged (moTAP) RIP3 construct with 2x FLAG and 2x Strep tags separated by a PreScission cut site. The purification scheme is diagrammed above (**Fig 2.1A**). Briefly, lysate is subjected to two arounds of affinity purification with FLAG and Streptactin pulldown. Following initial FLAG pulldown, the moTAP tag is cleaved at the PreScission site between FLAG and Strep and the eluate is collected for Streptactin precipitation. After the second round of IP, the bound protein is released by addition of desthiobiotin and the final complex is analyzed by Western blot. Expression of the construct was stable and can be readily picked up α-FLAG antibody in many cell lines, including kidney cell line 293T, fibrosarcoma L929, and fibroblast 3T3 cells (**Fig 2.1B**). Both FLAG and Strep tags were detectable; however, blotting with the Strep antibody often resulted in a significant level of background signal (data not shown) in the whole cell lysate so FLAG was used for verification of construct expression in subsequent experiments.

Though we were able to express to a high level the construct in both cell lines, the purification process proved to be inefficient. Initial FLAG pulldown of mo-TAP RIP3 (mtRIP3) revealed significant enrichment of the protein bound to beads (**Fig 2.1C**). Though some background signal from the isotype control was observed, the fold difference between the IP and isotype samples was still sufficient to conclude that the pulldown itself was fairly efficient.

However, when we tried to elute the protein off of the protein A/G beads by either addition of PreScission protease or a competitor of FLAG binding, 3x FLAG peptide, we were met with mixed results (**Fig 2.1C, D**). Upon addition of the protease, we no longer detect FLAG, which is expected as the FLAG tag is N-terminal to the cut site and thus should be cleaved off upon successful digestion. However, only a faint band was detected by Strep antibody, indicating the majority of the eluted protein was lost. Furthermore, we observed traces of the protease in the eluate (data not shown) at much higher levels than expected and than the eluted construct, which may potentially interfere with subsequent pulldown and purification. These results were repeated even for a low concentration of protease. Due to the inefficiency of the cleavage, we altered our strategy to adopt competition based elution of the immunoprecipitated construct.

High concentrations of 3x FLAG peptide led to increased levels of elution of moTAP RIP3 compared to protease digestion (**Fig 2.1D**). However, we still observed a significant amount of the tagged protein bound to the beads. We further subjected the eluate to pulldown with Streptavidin and a second round of elution with desthiobiotin and although we were able to observe a clear band corresponding to moTAP RIP3 in the final eluate, the signal was weak and again revealed that the majority of the protein remained bound to the beads (**Fig 2.1E**).

We tested the ability of our tagged protein to function and interact with partner proteins in necroptosis in L929 cells, which readily undergo TNF mediated necroptosis in the presence of the caspase 8 inhibitor zVAD-fmk (**Fig 2.1F**). We observed elevated cell death and co-interaction of RIP1 with moTAP RIP3 upon treatment with TNF and zVAD in stably transduced L929s. We also saw some interaction in untreated samples, though this result is expected as L929 cells display a basal level of necroptosis from autocrine TNF production[87].

We aimed to optimize a protocol for transduction of activated primary T cells, which are resistant to introduction of foreign DNA by most transfection methods. The end purpose is to establish a workflow for mtRIP3 complex purification to identify binding partners of RIP3 in T cell activation induced necroptosis. Although generation of transgenic mice expressing mtRIP3 may be eventually necessary to accommodate the large scale of the protein isolation, we first wanted to determine whether mtRIP3 had any adverse effects on T cell activation. We column purified T cells from the spleen and lymph nodes of twelve weeks old B6 mice. They were activated by crosslinking antibodies to CD3 and CD28 in the presence of IL-2, which prolongs their survival and provides us with an adequate time window for transduction and expression of mtRIP3. T cells activated in this manner were still able to undergo necroptosis, as Nec-1 rescued a portion of these cells from death, resulting in cell expansion beyond the limit of seven days in the absence of IL-2 (**Fig 2.2A**). We then infected these cells with pMSCV GFP mtRIP3 retrovirus concentrated from Px producer cell lines and were able to achieve on average 20-25% transduction efficiency as revealed by flow cytometry (**Fig 2.2B**). We did not observe significant differences in cell viability between the transduced and control cells, which may reflect the relatively low level of expression (data not shown). However, when we performed a co-IP with RIP1 on lysate from transduced T cells 120 hours post initial activation, we were unable to detect interaction between mtRIP3 and RIP1 (**Fig 2.2C**). While we saw expression of both RIP1 and RIP3 in the input and were able to specifically capture the majority of RIP1 protein by IP (IP:RIP1 bead lane vs IP:IgG2a bead lane), we did not see any RIP3 pulled down along with RIP1 (IP:RIP1 bead). Instead, almost all of the RIP3 we detected remained in the unbound supernatant (IP:RIP1 sup).

To determine whether the relatively weak expression of mtRIP3 in T cells may prevent us from observing the expected interaction, as we previously were able to verify in L929 cells, we

used an N-terminal FLAG tagged RIP3 expressed under a strong CMV promoter compared to one expressed under a weaker viral promoter for co-IP comparisons. We introduced the constructs into NIH-3T3 cells, which also readily undergo necroptosis in the presence of TNF, zVAD, and RIP3, and harvested the lysates 48 hrs post initiation of necroptosis for pulldown with RIP1 (**Fig 2.2D, E**). In the strong CMV promoter transfected samples, we saw a heavy FLAG band in both the untreated and treated IP samples (IP:RIP1 bead, +/- TNF+zVAD Fig 2.2D) and none in the isotype controls, with a greater signal in the TNF+zVAD samples, indicating specific co-IP of FLAG tagged RIP3 with RIP1. We observed two bands upon detection with FLAG antibody in all lanes in this experiment but only captured the top band (IP:bead lanes), which may correspond to phosphorylated RIP3 induced by activation of necroptosis. We did not observe a double FLAG band when we expressed RIP3 under a weaker promoter (Input lanes, bottom panel, Fig 2.2E). Indeed, despite successful pulldown with RIP1 (IP:RIP1 lanes, top panel), we detected no FLAG expression in the co-IP (IP:RIP1 lanes, bottom panel). Thus, a high amount of mtRIP3 expression appears to be crucial for allowing for complex formation and may point to the improved feasibility of a transgenic mouse approach over *in vitro* transduction.

Discussion

We generated a moTAP RIP3 construct to identify members of the RIP3 interacting complex in activated T cells as much of the biochemical details in this pathway - both the upstream inducers as well as the downstream effectors - are unknown. We were able to express a functional construct in various cell lines such as L929s and NIH-3T3s and was able to detect co-interaction of moTAP RIP3 with RIP1 and presumably other members of the canonical TNF-induced necrosome when it is expressed at high levels. We were also to specifically isolate the tagged protein through a two-step purification process. However, the amount of protein we eluted was extraordinarily low and not sufficient for analysis by mass spectrometry, despite a relatively large amount of cells and lysate used for the initial pulldown (~10-20 mg of protein). The key bottleneck of the process lay in the inefficiency of the methods (protein cleavage and peptide competition) to release bound protein after pulldown, resulting in loss of 80-90% of the precipitated protein despite extensive optimization of buffers and concentrations of reagents used. Thus, given the limits of the elution process, we anticipate requiring a much larger volume of cells for protein expression, which may necessitate altering the cell lines, vectors, and general approach used for isolation of the complex.

We also attempted to express mtRIP3 in activated T cells but were only somewhat successful in that regard. T cells are by nature difficult to manipulate genetically due to their short lifespan *in vitro*, their resistance to most methods of DNA delivery such as transfection and transduction with a majority of vectors, and the tight timing of many of the signaling events. While we were able to achieve a degree of efficiency in our transduction process that allowed us to visualize the expressed protein and perform a co-IP from these transduced cells, we were unable to detect the expected binding partners of RIP3, including RIP1. We later determined that the relatively low level of construct expression in T cells may be the culprit, as varying the strength of the promoter for mtRIP3 expression in NIH-3T3s drastically affected the ability of the construct to interact with RIP1, with almost no interaction detectable with a weak promoter. Together, these results suggest that the moTAP tag does not appear to interfere with the ability of RIP3 to interact with its binding partners an that the isolation of the expressed protein is highly specific. However, the efficiency of the process overall is so low that generation of a transgenic

mouse model may be more suited over an *in vitro* approach for using this method to identify binding partners of RIP3 in activated T cells, helping greatly in circumventing issues with expression as well as obtaining large cell volumes to combat the inefficiency of the elution process.

FIGURE LEGENDS
FIGURE 2.1

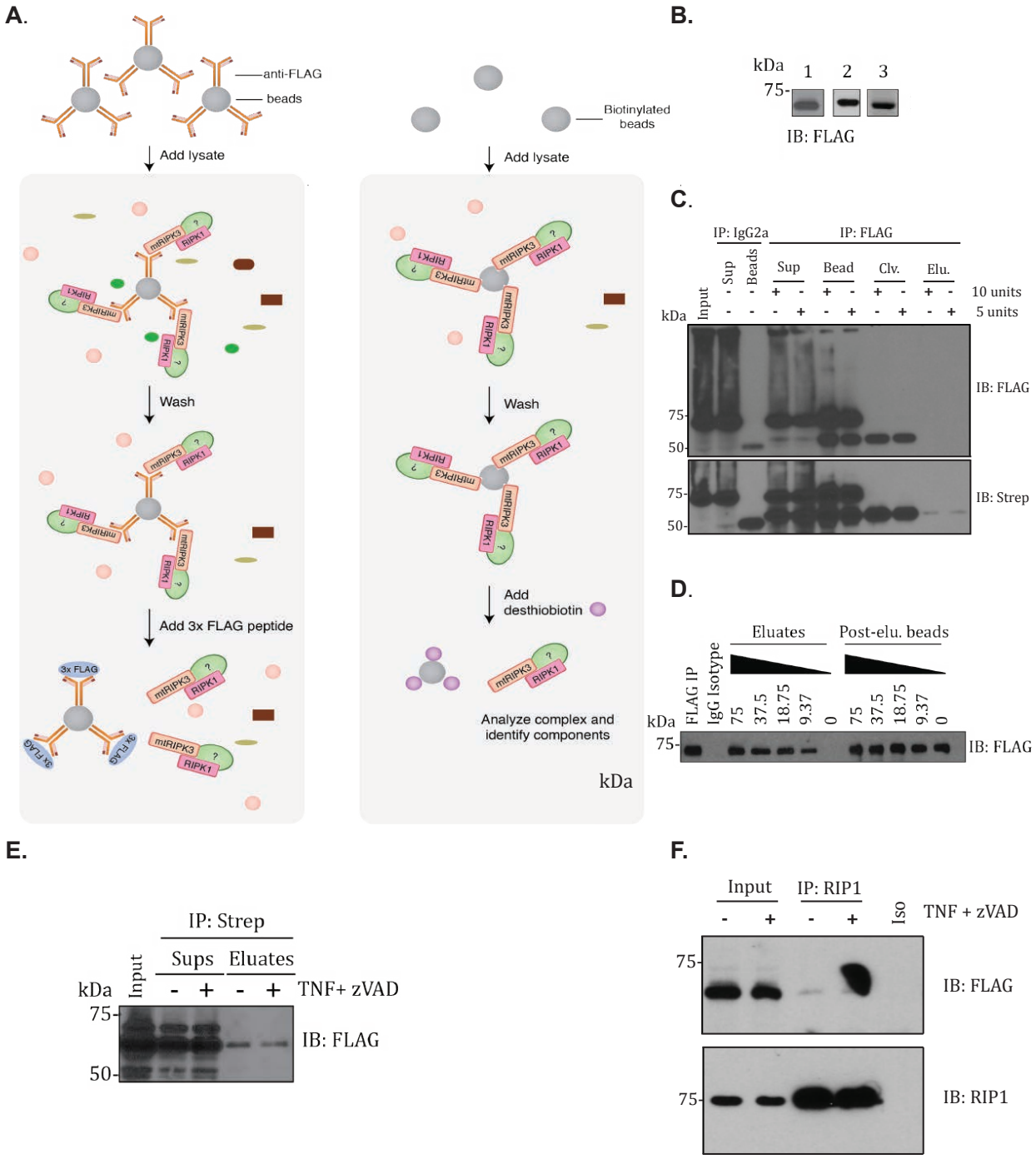

Figure 2.1 Generation and purification of moTAP RIP3 construct. A) Schematic of moTAP purification workflow. Lysate containing moTAP (2xFLAG-PreScss-2xStrep) tag is first affinity purified by α-FLAG IP. The bound protein is then eluted by cleavage with PreScission, a modified human rhinovirus 3C protease, or competitive binding with 3x FLAG peptide. The released protein is then subjected to a second round of affinity purification by Streptactin pulldown and subsequent elution with desthiobiotin before it is concentrated and denatured with 4x SDS for WB analysis. B) Expression of moTAP RIP3 construct in 1) 293T 2) 3T3 and 3) L929 cell lines. 293T and 3T3 cells were transfected with pCI or pcDNA3.1 moTAP-RIP3. L929 cells were transduced with pMSCV moTAP-RIP3 virus produced from Phoenix cells. Expression 24 hours post-transfection or 72 hours post-transduction was analyzed by SDS denaturation of cell lysate and Western blotting. C) PreScission protease elution of moTAP RIP3 at high and low concentrations. Lysate from transfected 293T cells were subjected to FLAG IP as per above. PreScission protease was added at the indicated amounts in cleavage buffer and incubated with bound complex. Protein was eluted by brief centrifugation. Sup, supernatant containing uncaptured protein; bead, protein A/G beads post-IP; clv., protein A/G beads post-cleavage with PreScission; elu., eluate post-cleavage. D) Elution of moTAP RIP3 following FLAG IP with titration of 3x FLAG peptide. Lysate was collected from L929 cells stably transduced with pMSCV moTAP-RIP3 and FLAG antibody was used for pulldown. The captured complex was then eluted from protein A/G beads by addition of varying concentrations (μg/mL) of 3x FLAG peptide. E) Strep elution of moTAP RIP3 following Streptavidin pulldown of lysate from stably transduced L929 cells. L929 cells stably expressing pMSCV moTAP-RIP3 were harvestedand lysed in standard IP buffer described previously. Streptactin sepharose beads were added and the mixture was incubated overnight on an end-over-end rotor at 4ºC. Beads were collected and transferred to an elution column. desthiobiotin elution buffer diluted in water was added to the column, and incubated on a rotor. Eluate was collected by brief centrifugation and a portion was boiled with 4x SDS and analyzed by Western blotting. F) Co-IP of moTAP RIP3 with RIP1 in stably transduced L929 cells upon addition of TNF+zVAD. Stably transduced L929 cells were treated with 60 ng/mL of recombinant mouse TNF and 20 μg/mL of zVAD and then collected 24 hours post-treatment. FLAG IP was performed as indicated above and beads were boiled and denatured for Western blot analysis.

FIGURE 2.2

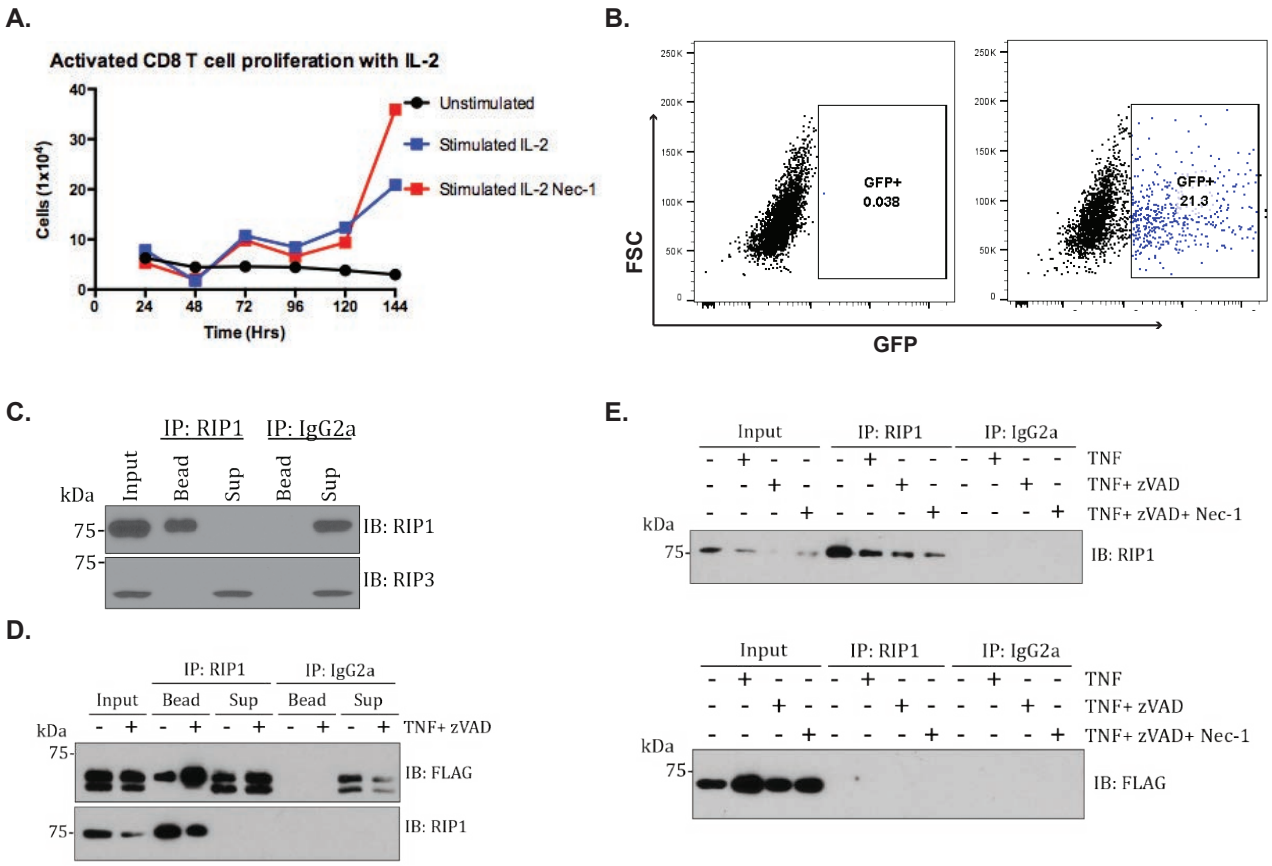
A.
Activated CD8 T cell proliferation with IL-2
Cells (1x10⁴)
Time (Hrs)
Unstimulated
Stimulated IL-2
Stimulated IL-2 Nec-1
B.
FSC
GFP
GFP+
0.038
GFP+
21.3
C.
IP: RIP1
IP: IgG2a
Input
Bead
Sup
Bead
Sup
kDa
75
IB: RIP1
75
IB: RIP3
D.
IP: RIP1
IP: IgG2a
Input
Bead
Sup
Bead
Sup
kDa
TNF+ zVAD
75
IB: FLAG
75
IB: RIP1
E.
Input
IP: RIP1
IP: IgG2a
TNF
TNF+ zVAD
TNF+ zVAD+ Nec-1
kDa
75
IB: RIP1
Input
IP: RIP1
IP: IgG2a
TNF
TNF+ zVAD
TNF+ zVAD+ Nec-1
kDa
75
IB: FLAG

Fig. 2.2 Infection and co-immunoprecipitation of moTAP RIP3 in activated T cells. A) Activation and rescue from necroptosis of B6 T cells in presence of IL-2. We stimulated purified T cells from six to week old B6 mice with CD3/CD28 antibody in the presence of of IL-2. Live cells were counted by Trypan blue. B) GFP expression of transduced T cells (right) compared to uninfected T cells (left). T cells were purified and activated with CD3/CD28 antibody stimulation for 72 hours prior to transduction. pMSCV moTAP-RIP3 virus generated by transfection of Phoenix cells was used to infect mouse T cells. GFP expression was monitored daily by microscopy and quantitatively analyzed 5-7 days post-infection by FACS. C) Co-IP of mtRIP3 infected cells with RIP1 120 hrs post activation. T cells were infected as per above and lysate was collected three days post-transduction and subjected to pulldown with RIP1 antibody. Samples were boiled and analyzed by Western blotting. D) Co-IP of FLAG tagged RIP3 expressed under a strong CMV promoter in TNF+zVAD treated NIH-3T3 cells with RIP1. NIH-3T3 cells were transfected with tagged RIP3. 24 hours later, TNF and zVAD was added at previously indicated concentrations and lysates were collected between 24-48 hours post-treatment and subjected to RIP1 IP. Sup, supernatants containing unbound protein. E) Co-IP of mtRIP3 with RIP1 in TNF+zVAD treated NIH 3T3 cells. NIH-3T3 cells were transduced with pMSCV moTAP-RIP3 and treated 72 hours post-infection with combinations TNF, zVAD, and Nec-1. Lysates were collected 24-48 hours after treatment and RIP1 IP was performed.

REFERENCES

1. Pardoll, D. M. The blockade of immune checkpoints in cancer immunotherapy. *Nat. Rev. Cancer* **12,** 252–264 (2012).
2. Mellman, I., Coukos, G. & Dranoff, G. Cancer immunotherapy comes of age. *Nature* **480,** 480–489 (2011).
3. Smith-garvin, J. E., Koretzky, G. A. & Jordan, M. S. T Cell Activation. *Annu. Rev. Immunol.* **27,** 591-619 (2009).
4. Elmore, S. Apoptosis : A Review of Programmed Cell Death. *Toxico Pathol.* **35,** 495–516 (2007).
5. Kaiser, W. J. *et al.* RIP3 mediates the embryonic lethality of caspase-8-deficient mice. *Nature* **471,** 368–372 (2011).
6. Osborn, S. L. *et al.* Fas-associated death domain (FADD) is a negative regulator of T-cell receptor – mediated necroptosis. *Proc Natl Acad Sci* **107,** 1–6 (2010).
7. Holler, N. *et al.* Fas triggers an alternative , caspase-8 – independent cell death pathway using the kinase RIP as effector molecule. *Nat Immunol.* **1,** 489–495 (2000).
8. Degterev, A. *et al.* Chemical inhibitor of nonapoptotic cell death with therapeutic potential for ischemic brain injury. *Nat Chem Biol* **1,** 112-119 (2013).
9. Gong, Y. *et al.* Biological events and molecular signaling following MLKL activation during necroptosis during necroptosis. *Cell Cycle* **16,** 1748–1760 (2017).
10. Wang, H. *et al.* Article Mixed Lineage Kinase Domain-like Protein MLKL Causes Necrotic Membrane Disruption upon Phosphorylation by RIP3. *Mol. Cell* **54,** 133–146 (2014).
11. Powles, T. *et al.* activity in metastatic bladder cancer. *Nature* **515,** 558–562 (2014).
12. Phan, G. Q. *et al.* Cancer regression and autoimmunity induced by cytotoxic T lymphocyte-associated antigen 4 blockade in patients with metastatic melanoma. *Proc Natl Acad Sci* **100,** 8372-8377 (2003).
13. Leach, D. R., Krummel, M. F. & Allison, J. P. Enhancement of Antitumor Immunity by CTLA-4 Blockade *Science* **271,** 1734–1736 (2017).
14. Hwu, W. *et al.* Safety and Activity of Anti–PD-L1 Antibody in Patients with Advanced Cancer. *N Engl J Med* **366,** 2455–2465 (2012).
15. Tenev, T. *et al.* The Ripoptosome , a Signaling Platform that Assembles in Response to Genotoxic Stress and Loss of IAPs. *Mol. Cell* **43,** 432–448 (2011).
16. Robinson, N. *et al.* Type I interferon induces necroptosis in macrophages during infection with Salmonella enterica serovar Typhimurium. *Nat Immunol* **13,** 954-962 (2012).
17. Newton, K. & Manning, G. Necroptosis and Inflammation. *Annu Rev Biochem* **85,** 743-63 (2016).
18. Vanlangenakker, N., Berghe, T. Vanden & Vandenabeele, P. Many stimuli pull the necrotic trigger , an overview. *Cell Death Differ* **19,** 75–86 (2011).
19. Ashkenazi A., and Dixit, V. M. Apoptosis control by death and decoy receptors. *Cell Regul.* **1,** 255–260 (1999).
20. Hsu, H., Shu, H., Pan, M. & Goeddel, D. V. TRADD – TRAF2 and TRADD – FADD Interactions Define Two Distinct TNF Receptor 1 Signal Transduction Pathways. *Cell* **84,** 299–308 (1996).
21. Mcilwain, D. R., Berger, T. & Mak, T. W. Caspase Functions in Cell Death and Disease. *Cold Spring Harb Perspect Biol* **5,** 1-29 (2013).

22. Oberst, A. & Green, D. R. It cuts both ways: reconciling the dual roles of caspase 8 in cell death and survival. *Nat Rev Mol Cell Biol* **12,** 757–763 (2011).
23. Chang, D. W. *et al.* c-FLIP L is a dual function regulator for caspase-8 activation and CD95-mediated apoptosis. *EMBO J* **21,** 3704-3714 (2002).
24. Safa, A.R. c-FLIP, a master anti-apoptotic regulator. *Exp Oncol* **34,** 176–184 (2012).
25. Ram, D. R. *et al.* Balance between short and long isoforms of cFLIP regulates Fas-mediated apoptosis in vivo. *Proc Natl Acad Sci* **113,** 1606-1611 (2016).
26. Tseveleki, V. *et al.* Cellular FLIP (long isoform) overexpression in T cells drives Th2 effector responses and promotes immunoregulation in experimental autoimmune encephalomyelitis. *J Immunol* **173,** 6619-6626 (2004).
27. Almagro, M. C. De *et al.* Coordinated ubiquitination and phosphorylation of RIP1 regulates necroptotic cell death. *Cell Death Differ.* **24,** 26–37 (2016).
28. Wertz, I. E. & Dixit, V. M. Signaling to NF- k B : Regulation by Ubiquitination. *Cold Spring Harb Perspect Biol* **2,** 1–19 (2010).
29. Donnell, M. A. O., Legarda-addison, D., Skountzos, P., Yeh, W. C. & Ting, A. T. Ubiquitination of RIP1 Regulates an NF- k B-Independent Cell-Death Switch in TNF Signaling. *Curr Biol* **17,** 418–424 (2007).
30. Lawrence, C. P. & Chow, S. C. FADD deficiency sensitises Jurkat T cells to TNF- a - dependent necrosis during activation-induced cell death. *FEBS* **579,** 6465–6472 (2005).
31. Kaiser, W. J. *et al.* Toll-like Receptor 3-mediated necrosis via TRIF , RIP3 and MLKL. *JBC* **43,** 31268-31279 (2013).
32. Nguyen, T. & Russell, J. The regulation of FasL expression during activation-induced cell death (AICD). *Immunol* **103,** 426–434 (2001).
33. Refaeli, Y., Parijs, L. Van & London, C. A. Biochemical Mechanisms of IL-2 – Regulated Fas-Mediated T Cell Apoptosis. *Immunity* **8,** 615–623 (1998).
34. Marrack, P. & Kappler, J. Control of T cell viability. *Annu Rev Immunol* **22,** 765-787 (2004).
35. Porter, B. B. & Harty, J. T. The Onset of CD8 ∂ -T-Cell Contraction Is Influenced by the Peak of Listeria monocytogenes Infection and Antigen Display. *Infec Immun* **74,** 1528–1536 (2006).
36. Strasser, A. & Pellegrini, M. T-lymphocyte death during shutdown of an immune response. *Trends Immunol.* **25,** 610–615 (2017).
37. Prlic, M., Hernandez-hoyos, G. & Bevan, M. J. Duration of the initial TCR stimulus controls the magnitude but not functionality of the CD8 + T cell response. *JEM* **203,** 2135–2143 (2006).
38. Moreau, D. *et al.* Resource Dissecting T Cell Contraction In Vivo Using a Genetically Encoded Reporter of Apoptosis. *Cell Rep* **2,** 1438–1447 (2012).
39. Prlic, M. & Bevan, M. J. Exploring regulatory mechanisms of CD8 T cell contraction. *Proc Natl Acad Sci* **105,** 16689-166984 (2008).
40. Onizawa, M. *et al.* The ubiquitin-modifying enzyme A20 restricts ubiquitination of the kinase RIPK3 and protects cells from necroptosis. *Nat Immunol* **16,** 618-627 (2015).
41. Shankaran, V. *et al.* IFN g and lymphocytes prevent primary tumour development and shape tumour immunogenicity. *Nature* **410,** 1107–1111 (2001).
42. Dunn, G. P., Old, L. J. & Schreiber, R. D. The immunobiology of cancer immunosurveillance and immunoediting. *Immunity* **2,** 137-48 (2004).
43. Coulie, P. G., Eynde, B. J. Van Den & Bruggen, P. Van Der. Tumour antigens recognized

by T lymphocytes : at the core of cancer immunotherapy. *Nat Rev Cancer* **14,** 135–146 (2014).
44. Mahoney, K. M., Rennert, P. D. & Freeman, G. J. Combination cancer immunotherapy and new immunomodulatory targets. *Nat Rev Drug Discov* **14,** 561-584 (2015).
45. Rosenberg, S. A. & Restifo, N. P. Adoptive cell transfer as personalized immunotherapy for human cancer. *Science* **348,** 62-68 (2015).
46. Rabinovich G. A., Gabrilovich D., and Sotomayor E. M. Immunosuppressive strategies that are mediated by tumor cells. *Annu Rev Immunol* **25,** 267–296 (2007).
47. Chaudhary, B. & Elkord, E. Regulatory T Cells in the Tumor Microenvironment and Cancer Progression: Role and Therapeutic Targeting. *Vaccines* **4,** 28 (2016).
48. Nishikawa, H., Sakaguchi, S., Cd, F. & Treg, T. ScienceDirect Regulatory T cells in cancer immunotherapy. *Curr. Opin. Immunol.* **27,** 1–7 (2014).
49. Schietinger, A. & Greenberg, P. D. Tolerance and exhaustion: defining mechanisms of T cell dysfunction. *Trends Immunol.* **35,** 51–60 (2017).
50. Crespo, J., Sun, H., Welling, T. H., Tian, Z. & Zou, W. T cell anergy , exhaustion , senescence , and stemness in the tumor microenvironment. *Curr. Opin. Immunol.* **25,** 214–221 (2013).
51. Pauken, K. E. & Wherry, E. J. Overcoming T cell exhaustion in infection and cancer. *Trends Immunol.* **36,** 265–276 (2017).
52. Schietinger, A. *et al.* Tumor-specific T cell dysfunction is a dynamic antigen-driven differentiation program initiated early during tumorigenesis. *Immunity* **45,** 389–401 (2016).
53. Zarour, H. M. Reversing T-cell dysfunction and exhaustion in cancer. *Clin Cancer Res* **22,** 1856–1864 (2017).
54. Lussier, D. M., Johnson, J. L., Hingorani, P. & Blattman, J. N. Combination immunotherapy with α -CTLA-4 and α -PD-L1 antibody blockade prevents immune escape and leads to complete control of metastatic osteosarcoma. *J. ImmunoTherapy Cancer*. **3,** 1-11 (2015).
55. Motz, G. T. *et al.* Tumor endothelium FasL establishes a selective immune barrier promoting tolerance in tumors. *Nat. Med.* **20,** 607 (2014).
56. Hargadon, K. M. Tumor-altered dendritic cell function: Implications for anti-tumor immunity. *Front. Immunol.* **4,** 1–13 (2013).
57. Cabillic, F. *et al.* Interleukin-6 and vascular endothelial growth factor release by renal cell carcinoma cells impedes lymphocyte-dendritic cell cross-talk. *Clin. Exp. Immunol.* **146,** 518–523 (2006).
58. Caestecker, M. P. De, Piek, E. & Roberts, A. B. in Cancer. **92,** 420–425 (2000).
59. Tanchot, C. *et al.* Tumor-infiltrating regulatory T cells: Phenotype, role, mechanism of expansion in situ and clinical significance. *Cancer Microenviron.* **6,** 147–157 (2013).
60. Thomas, D. A. & Massagué, J. TGF-beta directly targets cytotoxic T cell functions during tumor evasion of immune surveillance. *Cancer Cell* **8,** 369–380 (2017).
61. Juneja, V. R. *et al.* PD-L1 on tumor cells is sufficient for immune evasion in immunogenic tumors and inhibits CD8 T cell cytotoxicity. *J. Exp. Med.* **214,** 895–904 (2017).
62. Chen, L. & Han, X. Anti – PD-1 / PD-L1 therapy of human cancer : past , present , and future. *J. Clin. Invest.* **125,** 3384–3391 (2015).
63. Wing, K. *et al.* CTLA-4 Control over Foxp3 + regulatory T cell function. *Science* **322,** 271–276 (2008).

64. Brenner, D., Krammer, P. H. & Arnold, R. Concepts of activated T cell death. *Crit. Rev. Oncol. Hematol.* **66,** 52–64 (2008).
65. Takahashi, N. *et al.* Necrostatin-1 analogues: Critical issues on the specificity, activity and in vivo use in experimental disease models. *Cell Death Dis.* **3,** e437-10 (2012).
66. Schock, S. N. *et al.* Induction of necroptotic cell death by viral activation of the RIG-I or STING pathway. *Cell Death Differ.* **24,** 615–625 (2017).
67. Upton, J. W., Kaiser, W. J. & Mocarski, E. S. DAI/ZBP1/DLM-1 complexes with RIP3 to mediate virus-induced programmed necrosis that is targeted by murine cytomegalovirus vIRA. *Cell Host Microbe* **11,** 290–297 (2012).
68. Newton, K., Sun, X. & Dixit, V. M. Kinase RIP3 is dispensable for normal NF-kappa Bs, signaling by the B-cell and T-cell receptors, tumor necrosis factor receptor 1, and Toll-like receptors 2 and 4. *Mol. Cell. Biol.* **24,** 1464–1469 (2004).
69. Chen, D. S. & Mellman, I. Oncology meets immunology: The cancer-immunity cycle. *Immunity* **39,** 1–10 (2013).
70. Finn, O. J. Cancer Immunology. *N. Engl. J. Med.* **358,** 2704–2715 (2008).
71. Hartmann, B. M., Albrecht, R. A., Marjanovic, N. & Sealfon, S. C. Suppression of dendritic cell necroptosis by pandemic influenza virus. *J. Immunol.* **196,** 78 (2016).
72. Li, Z. *et al.* Tissue damage negatively regulates LPS-induced macrophage necroptosis. *Cell Death Differ.* **23,** 1428–1447 (2016).
73. Weinlich, R., Oberst, A., Beere, H. M. & Green, D. R. Necroptosis in development, inflammation and disease. *Nat. Rev. Mol. Cell Biol.* **18,** 127–136 (2017).
74. Chan, F. K.-M., Luz, N. F. & Moriwaki, K. Programmed necrosis in the Cross Talk of Cell Death and Inflammation. *Annu. Rev. Immunol.* **33,** 79–106 (2015).
75. Schock, S. N., Young, J. A., He, T. H., Sun, Y. & Winoto, A. Deletion of FADD in macrophages and granulocytes results in RIP3- and MyD88-dependent systemic inflammation. *PLoS One* **10,** 1–14 (2015).
76. Young, J. A., He, T. H., Reizis, B. & Winoto, A. Commensal Microbiota are Required for Systemic Inflammation Triggered by Necrotic Dendritic Cells. *Cell Rep.* **3,** 1932–1944 (2013).
77. Safa, A. R. Roles of c-FLIP in Apoptosis, Necroptosis, and Autophagy. *J. Carcinog. Mutagen.* **Suppl 6,** 3 (2013).
78. Tsuchiya, Y., Nakabayashi, O. & Nakano, H. FLIP the Switch: Regulation of Apoptosis and Necroptosis by cFLIP. *Int. J. Mol. Sci.* **16,** 30321–30341 (2015).
79. Vandenabeele, P., Galluzzi, L., Vanden Berghe, T. & Kroemer, G. Molecular mechanisms of necroptosis: an ordered cellular explosion. *Nat. Rev. Mol. Cell Biol.* **11,** 700-714 (2010).
80. Galluzzi, L., Kepp, O., Chan, F. K.-M. & Kroemer, G. Necroptosis: Mechanisms and Relevance to Disease. *Annu. Rev. Pathol. Mech. Dis.* **12,** 103–130 (2017).
81. Schworer, S. A. *et al.* Toll-like receptor-mediated down-regulation of the deubiquitinase cylindromatosis (CYLD) protects macrophages from necroptosis in wild-derived mice. *J. Biol. Chem.* **289,** 14422–14433 (2014).
82. Lin, J.-X. & Leonard, W. J. The role of Stat5a and Stat5b in signaling by IL-2 family cytokines. *Oncogene* **19,** 2566-2576 (2000).
83. Bashant, K. R. Necroptosis of Glycolytic Dendritic Cells Enhances Activation of Gamma Delta T Cells. *UVM Thesis* **96,** 1-26 (2016).
84. Huang, C.-Y., Kuo, W.-T., Huang, Y.-C., Lee, T.-C. & Yu, L. C. H. Resistance to hypoxia-induced necroptosis is conferred by glycolytic pyruvate scavenging of

mitochondrial superoxide in colorectal cancer cells. *Cell Death & Dis.* **4,** e622 (2013).
85. Chang, C.-H. *et al.* Posttranscriptional Control of T Cell Effector Function by Aerobic Glycolysis. *Cell* **153,** 1239–1251 (2017).
86. Gerlach, B. *et al.* Linear ubiquitination prevents inflammation and regulates immune signalling. *Nature* **471,** 591-596 (2011).
87. Wu, Y.-T. *et al.* zVAD-induced necroptosis in L929 cells depends on autocrine production of TNFα mediated by the PKC–MAPKs–AP-1 pathway. *Cell Death Differ.* **18,** 26-37 (2010).
88. Li, J. *et al.* The RIP1/RIP3 necrosome forms a functional amyloid signaling complex required for programmed necrosis. *Cell* **150**, 339-350 (2012).
89. Selby, M. J. *et al.* Anti-CTLA-4 antibodies of IgG2a isotype enhance antitumor activity through reduction of intratumoral regulatory T cells. *Cancer Immunol Res* **1**, 32-42, (2013).